# Passive reactivity control with $^{10}$B burnable poison in the U-battery

Simon de Die

April 12, 2007

# Foreword

This thesis represents my graduation thesis for the Master in Applied Physics at Delft University of Technology. The thesis work was performed in the section Physics of Nuclear Reactors (PNR) of the faculty of Applied Sciences.

I would like to express my gratitude towards all the members of the section PNR for their help and support. Especially I would like to thank Wilfred van Rooijen and Sieuwert de Zwaan for their day to day help, support and explanations of the SCALE, PERL and MATLAB programs. As well I would like to thank Jan Leen Kloosterman for giving new ideas on problem approaches and critical comments, which challenged further investigation.

Simon de Die

Delft, April 2007

# Executive Summary

In this study the topic of passive reactivity control in the U-Battery has been investigated. The U-Battery is a small, liquid salt cooled reactor, which is transportable by road. There is a need for passive reactivity control as the design should not contain active control systems, like control rods. The reactivity in the U-Battery can be controlled by inserting burnable poison into the fuel kernel of TRISO particles. In this study boron was used as poison. The limits to the reactivity swing are a 1% deviation from the $k_{eff} = 1$ line. The method investigated is controlling the reactivity by applying an inhomogeneous distribution of poison between reactor zones.

A first approach towards the problem was doing a reverse calculation based on the perturbation theory. As interrelations between the different zones was not known the poison was distributed proportional to the product of the poison absorption cross section, the flux and the adjoint function. This distribution was chosen as it would give the most efficient burnup. The result of this calculation showed that efficient burnup is not favoured as boron needs to be "saved" for later timesteps.

As a second approach a parameter study was conducted towards the distribution of poison in different zones. By varying the atomic density of the poison in different zones, and later expanding the number of zones as a satisfying reactivity swing was not yet achieved, there was calculated which configuration would have the lowest reactivity swing. The shortening of fuel lifetime was calculated as well to see what the effect of reactivity control would be on this parameter. A reactivity swing of less than 1% was achieved. However the fuel lifetime is shortened with around 140 days by the configuration achieving this reactivity swing. When a twice as large core, with less enrichment, is used a swing just as low can be achieved without loss of lifetime.

The lowest reactivity swing is achieved when a high atomic density is inserted into a narrow outer zone, next to the reflector, the zone where the product of the flux with the adjoint function is highest. A small density is needed in some inner zones as well. The configuration hinted at a large poison density in the reflector. Poison in the reflector turned out to give good solutions for reactivity control as well, although the accuracy of these calculations needs to be verified.

# Contents

# Chapter 1

# Introduction

The subject chosen in this thesis is "Passive reactivity control in the U-battery using burnable poison". The U-Battery is a small, graphite moderated reactor design transportable by road. There have been several designs for small nuclear reactors in the Netherlands, for example ACACIA [Heek et al., 2004] and the building block reactor [Uitert, 2006]. The design used in this thesis is based on a TU Delft design [De Zwaan, 2007]. The special features of this reactor will be described in chapter 5.

The subject refers to reactivity control as well. Reactivity control in nuclear reactors is needed as the core at the beginning of life will have an over-reactivity. This over-reactivity will cause too much fission and, with this, too high core temperatures. High temperatures can cause core meltdown and spilling of radioactive products into the environment.

In nuclear reactors reactivity can be controlled in several ways. The most common method for reactivity control is the use of control rods [Duderstadt and Hamilton, 1976]. These rods are neutron absorbing rods which control the reactivity through an active feedback system. During the lifetime of a reactor these rods are inserted in the core in case of over-reactivity and extracted out of the core in case of under-reactivity [Talamo, 2006] to compensate for fuel burnup and fission products buildup. In PWR's control rods are usually combined with reactivity control by soluble boron in the coolant [Duderstadt and Hamilton, 1976].

The aim of this thesis is to find a general solution method that is applicable for all nuclear reactors in general. The solution consists of a method to design a passive reactivity control. In this thesis a choice has been made to use burnable poison to control the reactivity. This poison consists of a nuclide with a large absorption cross section, which after the absorption of a neutron (and possibly the emission of another new particle), has a low absorption cross section. In figure 1.1 several poison absorption cross sections are shown. In this thesis boron, B-10, was chosen as poison as this is the most common poison used for reactivity control.

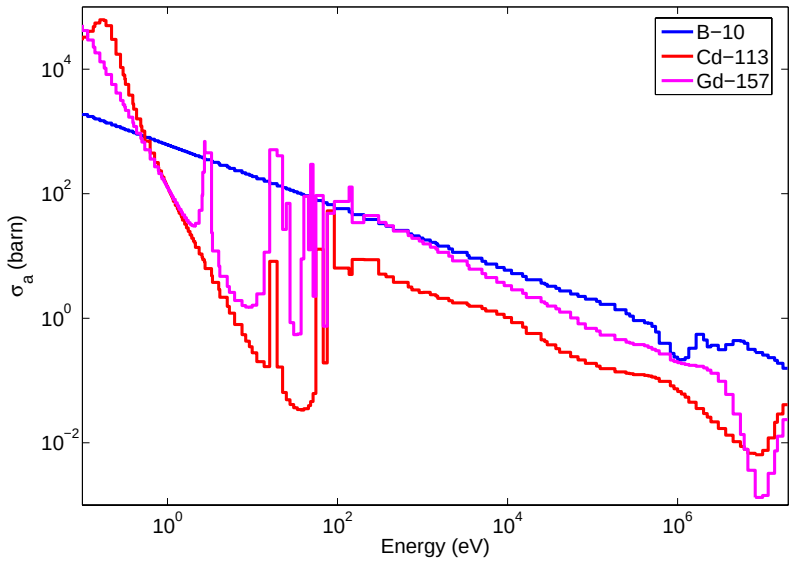


Figure 1.1: Microscopic absorption cross section for different reactor poisons

The poison in a reactor can be distributed in several ways which all have their characteristic influence on the reactivity. In some studies enriched burnable poison particles are investigated, for example by Dam [2000a] and Talamo [2006] or pure absorber-nuclide burnable poison particles by Kloosterman [2003]. The use of such particles gives two degrees design freedom, the radius of the poison particle and the poison particle density in the core. With these particles a reactivity swing as low as 2% can be achieved [Kloosterman, 2003]. The disadvantages of the use of poison particles is the extra cost of fabricating enriched particles. Non-enriched particles are cheaper but diminish the self-shielding effects which are used as a design parameter. The number of non-enriched particles needed will be larger than the number of enriched particles, so it has to be analysed whether this option turns out to be cheaper.

In other studies burnable poison distribution in the reflector were studied [Dam, 2000b], [Heek et al., 2004]. With these configurations a reactivity swing below 5% can be achieved. This however is done by introducing boron in an inner reflector, which is not present in the chosen reactor concept. For the reactor concept it has not been decided yet if it will reuse its reflector in several life-cycles. Therefore this option has been kept open. When the reflector will be recycled re-introducing a poison in each cycle is very difficult.

A third way of introducing a burnable poison in the core is by dissolving the poison in the coolant [Duderstadt and Hamilton, 1976]. The advantage of this is that the poison density can be controlled in the core during the lifetime of the reactor by the amount of poison added to the coolant. The disadvantage of this is however that there needs to be designed a feedback system which controls the amount of poison inserted.

In this thesis it was selected to use different fuel zones with different boron concentrations. Each TRISO particle, a fuel kernel with layers of pyrolytic carbon and a silicon carbide layer, in a certain zone has the same composition. The natural boron is mixed homogeneously in the fuel, while keeping the uranium density the same. This makes the TRISO particle fabrication process more difficult but avoids the need for boron enrichment. This also avoids the need for a solution to fill the fuel matrices with particles with two different diameters (TRISO and poison particles).

This thesis focuses on achieving a low reactivity swing of the $k_{eff}$ (discussed in section 2.1) instead of the $k_{\infty}$, the multiplication factor not taking into account leakage, calculated in the papers mentioned above. The aim is to keep the fuel lifetime reduction as small as possible as well.

The outline of this report is as follows. Chapter 2 describes the problem which is faced in this thesis and discusses several methods to solve the problem. The following two chapters (3 and 4) discuss theories for solving the problem. Chapter 3 describes the pertubation theory and chapter 4 describes the importance function, the adjoint function. Chapter 5 describes the reactor mock-up and the burnup calculations used to model the reactor. In the following chapter (chapter 6) an attempt is made to use the reverse calculation described in chapter 3 with the use of the importance function. Chapter 7 discusses a parameter evaluation of the problem. In the following chapter several conclusions are drawn on the work conducted in this thesis. The final chapter discusses several topics and indicates in which areas future work needs to be done.

A summary of the different methods used in this thesis to calculate how a low reactivity swing can be achieved is given in table 1.1.

Table 1.1: Summary of the methods used in this thesis to find the ideal poison distribution with a low reactivity swing. The last column indicates whether a reactivity swing of less than 1% was found.

| Method | Section | Advantages | Disadvantages | Solution found |
|---|---|---|---|---|
| Reverse calculation based on perturbation theory | 3.2 | Analytical approach | Many interrelations not known | No |
| Reverse calculation with fixed poison distribution based on the product of flux adjoint and $\sigma_a$ | 6.2 | Gives insight into reactor behaviour | Depleted poison does not match fresh poison-load needed | No |
| Parameter study with poison in two, expanded to four, fuel zones | 7.1 | Relative short calculation time | Two and four degrees of design freedom | No[1] |
| Parameter study with poison in three, expanded to six, fuel zones | 7.2 | Three and six degrees of design freedom | Relative long calculation time | Yes |
| Parameter study with poison in one fuel zone and in the reflector | 7.4 | Short calculation time | Accuracy of calculations not yet verified | Yes |

[1]There was no solution for the core of 3 $m^3$ used throughout the report, but a solution for the larger core of 6 $m^3$, discussed in section 7.3 was found.

# Chapter 2

# Problem definition

## 2.1 K-effective

In nuclear reactors the long term reactivity has to be controlled in order to maintain the fission chain reaction. However reactivity has to be controlled as well on a short term to avoid fission reactions getting out of control [Hoogenboom and Dam, 1998]. Under- or over-reactivity is indicated with the effective multiplication factor, $k_{eff}$. The multiplication factor indicates the relation between the neutron production rate through fission and the neutron disappearance rate through absorption and leakage. In a homogeneous reactor [Hoogenboom and Dam, 1998] this is described by the formula

$$k_{eff} = \frac{\int_V \sum^n \nu\Sigma_{f,n}}{\int_V \sum^n \Sigma_{a,n}} \int_V \sum^n \frac{1}{1 + L_n^2 B_g^2} \tag{2.1}$$

in which the $\nu\Sigma_{f,n}$ is the appearance term (number of new neutrons per fission, $\nu$, times the macroscopic fission cross section), $\Sigma_{a,n}$ and $\frac{1}{1+L_n^2 B_g^2}$ are the disappearance terms (macroscopic absorption cross section and non-leakage term respectively). In a continuous energy spectrum the terms in equation 2.1 are integrated over all energies. In this thesis summations over n energy groups are used in stead of integrals as the burnup programs use a group-wise calculation method.For a constant power level $k_{eff}$ needs to be one; the fission rate does not increase or decrease. If the $k_{eff}$ is below one the chain reaction will decrease; there are not enough neutrons generated to keep the chain reaction running. When the $k_{eff}$ is above one, consecutive generations will have more fission reactions.

In literature and in this thesis several different reactivity expressions are used. All of these expressions are related to the $k_{eff}$ as they all are a particular eigenvalue to solve the criticality equation (equation 4.1). The expressions used are

$$\rho \equiv \frac{k_{eff} - 1}{k_{eff}} \tag{2.2}$$

$$\lambda = \frac{1}{k_{eff}} \tag{2.3}$$

where the reactivity $\rho$ is a measure for a deviation from a critical system with $k_{eff} = 1$ and $\lambda$ is the inverse of the eigenvalue used to balance the criticality equation.

## 2.2 Reactivity in U-Battery

As the U-Battery starts with a certain fuel composition, based on the parameters described in chapter 5, the $k_{eff}$ will not be one at the start of life of the reactor, it can only be one with extra neutron absorbers. The nominator in equation 2.1 is larger than the denominator. During the lifetime the neutron production will become smaller due to the burnup of U-235, the primary neutron source. The neutron loss will become larger as well due to parasitic behaviour towards neutrons of the fission products. At a constant temperature of 1073 °K the evolution of the $k_{eff}$ during the lifetime of the reactor with no reactivity control or with B-10 burnable poison is shown in figure 2.1. The calculations were done with KENOBURN (section 5.2) on a 4 $m^3$, graphite moderated core. The used fuel consists of 20% enriched TRISO particles in a matrix fuel assembly. From figure 2.1 it can be concluded that actions have to be taken in order to avoid the chain reaction to get out of control.

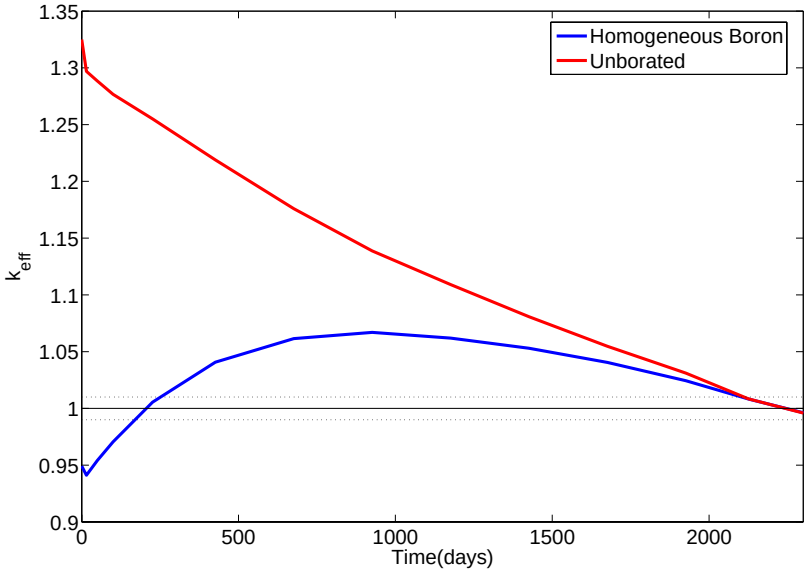


Figure 2.1: Evolution of the $k_{eff}$ during the lifetime of a 4 $m^3$, graphite moderated reactor, for a homogeneous borated and unborated core

## 2.3 Reactivity control

Controlling this over-reactivity is usually done by control rods in combination with borated coolant in PWR's [Duderstadt and Hamilton, 1976]. These rods are made of a neutron absorbing material. Due to this property the size of the denominator in equation 2.1 can be influenced by inserting or extracting the rods. These rods are used in a feed-back system which reacts on the power monitored in the reactor. As this is an active control system it has to be monitored, which results in extra operating costs.

Another option to control the reactivity in the reactor is the insertion of burnable poison. Burnable poison is made of a nuclide which has a large absorption cross section. After the absorption of a neutron the nuclide is transformed into another nuclide with a negligible absorption cross section. This property can be used by inserting the poison at the beginning of life to absorb excess neutrons and to lower the $k_{eff}$. During the lifetime of the reactor the poison will be burnt and have less influence on the $k_{eff}$. A possible disadvantage of the use of burnable poison is the leftover of poison at the end of reactor life, when too much poison is needed to compensate for over-reactivity at the beginning of life. In this stage the presence of poison is not necessary and only contributes to an earlier drop of $k_{eff}$ below one.

A natural physical reactivity control occurs through the Doppler effect [Duderstadt and Hamilton, 1976]. The Doppler effect describes the increase in absorption in the resonance region of U-238 (figure 4.3) because of the increase in resonance width through nucleus motion (the absorption cross section is based on relative velocity). Due to this Doppler effect the reactivity will decrease with increasing temperature as more neutrons are captured due to the larger resonance width. This gives the design freedom, that the $k_{eff}$ will converge towards one, when the $k_{eff}$ is within a certain range. The limits are set by the change in reactivity with temperature [Duderstadt and Hamilton, 1976]. A typical value for the temperature reactivity coefficient for a graphite moderated core is approximately given by:

$$\frac{d\rho}{dT} \simeq -7.10^{-5} K^{-1} \tag{2.4}$$

This limit sets the boundaries for acceptable values for which $k_{eff}$ converges to one. The reactor temperature is not allowed to fluctuate more than 150 °K. If the reactor gets too cold the efficiency in the heat exchanger will become very low. If the temperature gets too high material properties in the reactor will be pushed to their limits. This indicates that, when maintaining the fluctuation limit of 150 °K, a reactivity swing of maximum 1% is allowed around a $k_{eff}$ of one.

## 2.4 Scope of thesis

The scope of this thesis is to design a B-10 loading such that the reactor does not need control rods. This implicates that the $k_{eff}$ curve should be between 0.99 and 1.01, the

values between which the Doppler effect will compensate for excess reactivity and will have the $k_{eff}$ converge to one. The curve has to be between these values during the entire lifetime.

The creation of this curve will be achieved by using burnable poison to flatten the reactivity curve in figure 2.1 between the two black dotted lines (boundaries set above). The idea is to have the reactivity drop below 0.99 as late as possible during burnup in order to minimise the shortening of fuel lifetime. As a homogeneous distribution of poison will not be able to get the $k_{eff}$ curve between the wanted boundaries, as can be seen in figure 2.1, this thesis will aim to use different geometrical distributions of boron to achieve the goals. This implies the use of zones with different poison concentrations. The poison will be distributed homogeneously in each zone.

# Chapter 3

# Perturbation Theory

## 3.1 Theory

When a $k_{eff}$ curve is determined for a reactor at some point this line crosses the horizontal line $k_{eff} = 1$ at the end of fuel life. When this point is taken as a starting point the perturbation theory can be used. This theory assumes that when moving back along the curve the $\Delta\rho$ occurring is a small perturbation of the system.

The unperturbed multiplication equation of the system [Ott and Neuhold, 1985] can be described with

$$\mathbf{M}_0\Phi_0 = \lambda_0\mathbf{F}_0\Phi_0 \tag{3.1}$$

where the $\mathbf{M}$ operator denotes the neutron loss operator, the $\mathbf{F}$ operator denotes the neutron creation operator, $\Phi$ denotes the neutron flux and the subscript 0 denotes non perturbed, $\lambda$ is the eigenvalue balancing the system. For the perturbed system it holds:

$$\begin{aligned}
\mathbf{M}_p\Phi_p &= \lambda\mathbf{F}_p\Phi_p && (3.2)\\
\Delta\lambda &\equiv \lambda - \lambda_0 = -\Delta\rho && (3.3)\\
\Delta\mathbf{M} &\equiv \mathbf{M}_p - \mathbf{M}_0 && (3.4)\\
\Delta\mathbf{F} &\equiv \mathbf{F}_p - \mathbf{F}_0 && (3.5)\\
\Delta\Phi &\equiv \Phi_p - \Phi_0 && (3.6)
\end{aligned}$$

where the subscript p denotes perturbed.

Inserting equations 3.4 to 3.6 in the perturbed system 3.2 yields the equation

$$\mathbf{M}_p\Phi_0 = \lambda\mathbf{F}_p\Phi_0 - (\mathbf{M}_p - \lambda\mathbf{F}_p)\,\Delta\Phi \tag{3.7}$$

When equations 3.6 and 3.3 are inserted into the first term on the right-hand side this gives

$$\lambda\mathbf{F}_p\Phi_0 = \lambda\mathbf{F}_0\Phi_0 + \lambda_0\Delta\mathbf{F}\Phi_0 + \Delta\lambda\Delta\mathbf{F}\Phi_0 \tag{3.8}$$

An operator $\mathbf{A}^*$ is defined adjoint to the operator $\mathbf{A}$ when

$$(\mathbf{A}^* f, g) = (f, \mathbf{A} g) \tag{3.9}$$

for every $f(\mathbf{r})$ and $g(\mathbf{r})$ satisfying the boundary conditions that the functions $f$ and $g$ are zero on the core boundary and the inner product $(f, g)$ is defined as

$$(f, g) \equiv \int_V d^3 r f^*(\mathbf{r}) g(\mathbf{r}) \tag{3.10}$$

where $f^*(\mathbf{r})$ denotes the complex conjugate of $f(\mathbf{r})$ and $V$ is the core volume.

Equation 3.8, neglecting the second-order term, and the unperturbed system 3.1 are weighted with the adjoint function of the flux, $\Phi^*$, as weighting term and subtracted. This gives

$$(\Phi_0^*, [\Delta\mathbf{M} - \lambda_0 \Delta\mathbf{F}]\Phi_0) = \Delta\lambda\,(\Phi_0^*, \mathbf{F}_0\Phi_0) - (\Phi_0^*, [\mathbf{M}_p - \lambda\mathbf{F}_p]\Delta\Phi) \tag{3.11}$$

The weighting is done with the unperturbed adjoint function as this eliminates the first order term when the second term on the right hand side of equation 3.11 is written out in first-, second- and third-order terms. The second and third order terms are neglected. From this, the term containing the flux deformation due to the perturbation, $\Delta\Phi$ can be eliminated. The equation which is left after this elimination can be solved for $\Delta\rho$ and gives

$$\Delta\rho = \frac{(\Phi_0^*, [\lambda_0\Delta\mathbf{F} - \Delta\mathbf{M}]\Phi_0)}{(\Phi_0^*, \mathbf{F}_0\Phi_0)} \tag{3.12}$$

From this equation it is clear that the change in multiplication factor is due to the changes in the source and loss operators. When the starting point is a critical reactor $\lambda_0 = 1$ the perturbation of the criticality, due to changes in the creation operator ($\mathbf{F}$) can be balanced by inducing changes to the loss operator $\mathbf{M}$.

The SCALE [ORNL, 2005] software uses group wise approaches to describe the energy dependence of the cross sections. In that case the creation and loss operators can be seen as matrices. The loss matrix $\mathbf{M}$ is a matrix describing the loss of neutrons not only by absorption into a nuclide, but as well by scattering out of the energy group. The matrix has absorption cross sections on the diagonal and scatter cross sections in the upper triangle and zeros in the lower triangle as there is only down scattering. In the thermal region there is up scattering as well. Here the entries below the diagonal are non zero.

$$\mathbf{M} = \begin{pmatrix} \sigma_{a,i} & \sigma_{s,i\to j} & \sigma_{s,i\to k} & \cdots \\ 0 & \sigma_{a,j} & \sigma_{s,j\to k} & \cdots \\ 0 & 0 & \sigma_{a,k} & \cdots \\ \vdots & \vdots & \vdots & \ddots \end{pmatrix}$$

The $\mathbf{F}$ matrix is a diagonal matrix. On the diagonal are the probabilities of the creation of neutrons within a certain energy band multiplied by the average number of neutrons

created per fission ($\nu$).

$$\mathbf{F} = \begin{pmatrix} \nu\sigma_{f,i} & 0 & 0 & \dots \\ 0 & \nu\sigma_{f,j} & 0 & \dots \\ 0 & 0 & \nu\sigma_{f,k} & \dots \\ \vdots & \vdots & \vdots & \ddots \end{pmatrix}$$

## 3.2 Reverse calculation

The idea behind a reverse calculation is to use the perturbation theory in equation 3.12. From the point where the reactor is exactly critical a step back in time is taken which gives rise to a small $\Delta\rho$. This $\Delta\rho$ has to be brought back to zero at the point back in time as the reactor has to be exactly critical during the entire lifetime. Taking the step back in time changes the loss and creation operators as well. The creation operator has larger entries in an earlier point in time as there is more U-235 present and less fission products. This operator is determined up front by the enrichment of the reactor and is hard to influence (although manipulating uranium contents is possible but not favourable as this influences the life cycle of the reactor)

The only way to bring $\Delta\rho$ back to zero is by influencing the loss operator. By introducing a burnable poison into the reactor, the entries on the diagonal will become larger. However the upper triangle will have changes in entries as well as the introduced poison will have different scattering cross sections compared to the system.

When the new operator $\mathbf{M}$ is created by introducing the exact amount of poison the system balances again and it has a $k_{eff}$ of 1. Then a next step back in time is taken and the operator $\mathbf{M}$ is manipulated again with burnable poison. When these steps back in time reach the point in the burnup of the reactor just after the xenon and samarium poisoning for each point evaluated there might be an ideal operator $\mathbf{M}$. Comparing this operator with the operator for a burnup calculation the amount of poison needed in the reactor at that point can be seen.

Three problems arise when attempting this reverse calculation:

- Addition of poison in the reactor has an effect on the neutron spectrum. This creates the problem of not knowing how the leakage and (self)shielding will change by poison insertion. The SCALE software does a special XSDRNPM calculation in order to determine all these effects. As these effects cannot be predicted in advance, the influence of the insertion of poison on the system can not be predicted either. Therefore finding an analytical solution is impossible but a numerical solution can be found. Given these facts it is very hard to predict the outcome on the $\mathbf{M}$ operator of the insertion of some poison.

- The **M** matrices calculated in each step have to convert into each other by depletion (forward in time). Calculating this backwards in time needs knowledge of mother nuclides for each fission product. As the forming of fission products has a certain distribution according to the "Camel Curve" [Hoogenboom and Dam, 1998] it is impossible to know from which mother nuclide the new nuclide is a product.

- A third difficulty is the fact that in the burnup scripts the criticality equation, equation 3.1 is solved with each zone having different **M** and **F** operators which are interrelated. Therefore doing a back calculation needs to solve a system of criticality equations with an unknown interrelation. This unknown interrelation is caused by the fact that when changing the **M** operator, the leakage will change as well, which is input to another zone. However when certain assumptions are made about the poison distribution in the core, i.e. fixing the interrelations between the criticality equations for the zones a reverse calculation attempt using equation 3.12 can be undertaken. This is done in chapter 4.

# Chapter 4

# Adjoints

The method described in chapter 3 is difficult to use. In this chapter a new approach will be evaluated in order to simplify the method in chapter 3. This method is built on the physical properties of the adjoint function.

## 4.1 Theory

The neutron multiplication and criticality in a nuclear reactor are described [Ott and Neuhold, 1985] with the equation

$$\mathbf{M}\Phi = \lambda \mathbf{F}\Phi \tag{4.1}$$

This equation describes the relation between the migration and loss of neutrons for a certain energy ($\mathbf{M}\Phi$) and the source of neutrons described by the fission operator multiplied with the flux $\mathbf{F}\Phi$. The eigenvalue $\lambda$ is the term describing whether there is an equilibrium ($\lambda = 1$) or if there is an under or overproduction of neutrons.

From this equation the flux spectrum and distribution, $\Phi$, can be calculated and with that the multiplication factor $\lambda$ can be determined through an iterative process. The solution for this problem has been derived by means of a forward calculation. The same $\lambda$ can be calculated by an adjoint system by solving

$$\mathbf{M}^*\Phi^* = \lambda \mathbf{F}^*\Phi^* \tag{4.2}$$

This can be seen by taking the inner product of both sides of equation 4.1 with the adjoint, $\Phi^*$ (defined in equation 3.9). The new equation becomes:

$$(\Phi^*, \mathbf{M}\Phi) = \lambda\,(\Phi^*, \mathbf{F}\Phi) \tag{4.3}$$

Revolving both sides of the equations gives

$$(\Phi^*, \mathbf{M}\Phi) = (\mathbf{M}^*\Phi^*, \Phi) \tag{4.4}$$

$$(\Phi^*, \mathbf{F}\Phi) = (\mathbf{F}^*\Phi^*, \Phi) \tag{4.5}$$

Putting the right terms in equations 4.4 and 4.5 together

$$(\mathbf{M}^*\Phi^*, \Phi) = \lambda\,(\mathbf{F}^*\Phi^*, \Phi) \tag{4.6}$$

and eliminating the inner product with $\Phi$ finally gives the adjoint problem in equation 4.2.

The above proves that equations 4.1 and 4.2 will both give the same value for $\lambda$ when doing a criticality calculation. The solutions for $\Phi$ and $\Phi^*$ as functions of energy however will be different. The calculated $\Phi$ can be seen as a neutron flux. The solution given by the adjoint calculation, $\Phi^*$, cannot be seen as a neutron flux but is seen as an adjoint function, which is described as an *importance function* [Duderstadt and Hamilton, 1976].

By Duderstadt and Hamilton [1976] it is described that the adjoint function is a measure of how effective an absorber inserted at a certain position, $\mathbf{r_0}$, is in changing the reactivity of the core. The equation describing this is

$$\Phi^*(\mathbf{r}_0) \sim \frac{-\Delta\rho}{\alpha\Phi(\mathbf{r_0})} \tag{4.7}$$

where $\alpha\Phi(\mathbf{r_0})$ is the absorption rate at position $\mathbf{r_0}$. The value of $\alpha$ is the effective absorber strength and depends on the properties of the absorber nuclide used. From equation 4.7 it can be concluded that the magnitude of the product of the adjoint function with the forward flux determines the $\Delta\rho$ of the core when an absorber is inserted at a certain point $\mathbf{r}_0$.

## 4.2 Working the adjoints

The fact that the magnitude of the adjoint determines the influence on the neutronics in case of adding an absorber is quite usable (high adjoint, high absorption). As the U-Battery should have the longest possible lifetime, the ideal solution is found when all added boron is burnt up when the multiplication factor drops below 1 due to the burnup of the fuel. Then the fuel cycle length is not influenced by the addition of boron, but the depletion of the fuel only.

### 4.2.1 Adjoint Function Profile

In the SCALE software the XSDRNPM calculates the multiplication factor of the system by solving the eigenvalue equation 4.1 forward. The output of this calculation gives a $k_{eff}$ and a flux $\Phi$ per energy group. The profile is shown in figure 4.1a for the three different radial zones with equal volume and a 60 cm reflector described in figure 5.2a. The magnitudes of these fluxes can only be compared between the different zones as in this stage of computation the flux cannot be normalised on a defined value (profile before FLUX2POWER [figure 5.3]). However it can be seen that the thermal flux, as expected because of high moderation in the reflector, is higher for the reflector and the

outer zone.

XSDRNPM has the possibility to do criticality calculations by solving the adjoint problem[1]. The problem solved is the problem described in equation 4.2. The output given by this calculation consists of a $k_{eff}$, which is the same as calculated in the forward problem and the adjoint function, $\Phi^*$. The adjoint function is plotted in figure 4.1c. The resonances seen between 1 and 100 eV in the figure are the resonances of U-238. In the thermal region of the spectrum for all three fuel zones, the adjoint is higher than in the fast region. This is expected as an inserted neutron with thermal energy is more likely to cause a fission than a fast neutron. The fast neutron needs to be moderated and during moderation it has to pass the resonance region where there is a higher chance of absorption. The high adjoint value for fast neutrons in the reflector is caused by the higher moderation possibilities for a fast neutron. A fast neutron inserted in the reflector will not have to pass resonance regions while being moderated, so it will very likely become thermal and induce fission when leaking into the outer zone.

The relative height of the adjoint functions between the zones (figure 4.1c) is caused by the higher escape probability for the different zones. Going outward from the centre of the sphere the areas over which neutrons can diffuse to another zone and eventually out of the system becomes larger. It is therefore that the adjoint is lowest in the outer zone and highest in the inner zone. In the reflector it can be seen that in the thermal region the escape probability is even higher: this is expected as this is the outer region.

### 4.2.2 Adjoint Function U-Battery vs. PWR

The dip occurring beyond $10^7$ MeV does not occur in the adjoint function profile of a PWR as can be seen in figure 4.2. Calculations for the U-Battery without leakage (reflecting boundary) and without reflector and leakage give similar profiles for the adjoint function as in figure 4.1c. Therefore the dip must be a result of the fuel and cladding composition in the core. In figure 4.3 the cross sections of materials in the U-Battery are compared. The atomic density of carbon and oxygen combined is much higher (around a factor 100) than the density for U-238. The dominating absorption in the thermal and epithermal region will be due to U-238 as in this region the $\sigma_a$ of U-238 is a 1000-10000 times higher than the $\sigma_a$ for oxygen and carbon. In the very fast region the cross sections of oxygen and carbon will dominate as these are only a factor ten lower, while their atomic density is much higher. When the cross sections of C-12 and O-16 (figure 4.3) are compared with the adjoint function (figure 4.1c) it can be seen that the start of the dip in the adjoint function is at the same energy as the start of the jump in the C-12 cross section. From this it can be concluded that the dip is mainly caused by the graphite present in the core.

[1]The input is the same as for the forward problem except for one bit that indicates that the calculation has to be done adjoint.

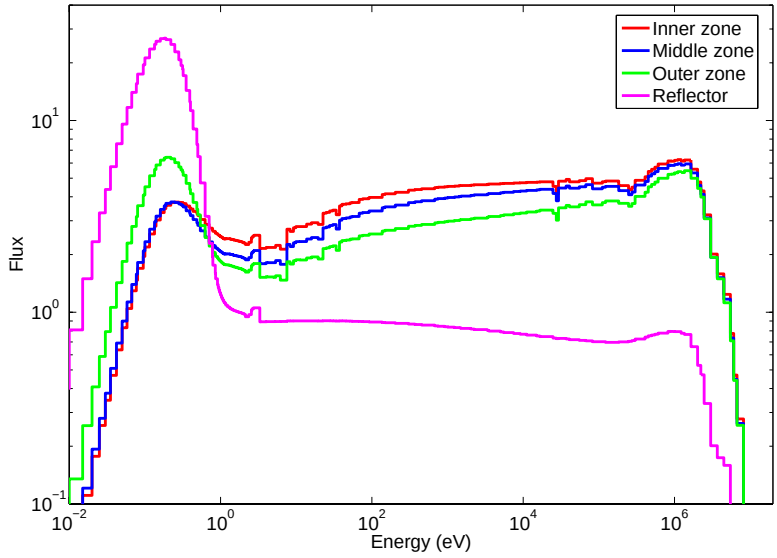


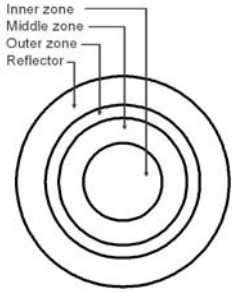


(a) Forward flux

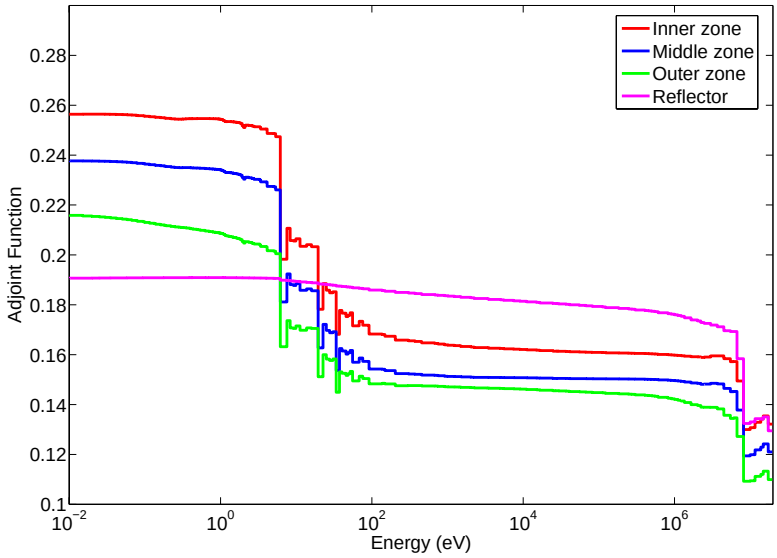


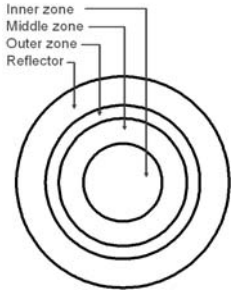


(c) Adjoint function

Figure 4.1: Flux and adjoint function profiles after 10 days (to include xenon and samarium poisoning) of burnup in a poison free reactor. Burnup calculations are done in three different spherical shell-zones of equal volume

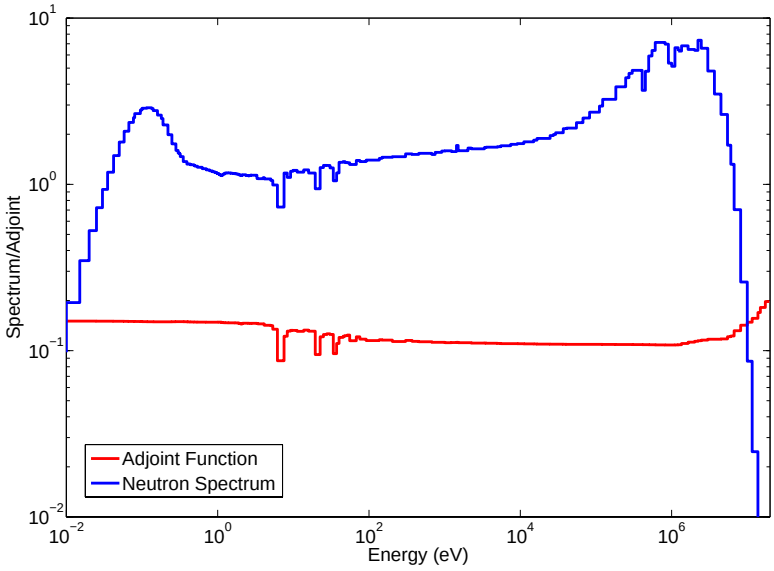


Figure 4.2: The adjoint function and flux for a PWR

### 4.2.3 Influence of poison on the $k_{eff}$

From equation 4.7 it follows that the largest adjoint yields the highest $\Delta\rho$, when a neutron with a certain energy is inserted. In the reactor there is a neutron flux present, with an energy distribution as described in figure 4.1a, which will cause a certain cumulative change in reactivity. When the flux is multiplied, mathematically it is the inner product, with the adjoint function (figure 4.1c) a measure for the change in reactivity can be seen for each region for different energies. This is shown in figure 4.4.

Which part of the spectrum dominates $\Delta\rho$ depends on the absorber as the absorber energy dependence is hidden in $\alpha$ in equation 4.7. When calculations are done with boron inserted in only one zone at a time it can be seen (figure 4.5) that the relative $|\Delta k_{eff}|$ matches the relative peak height in the thermal region; this is expected as the thermal region is the region in which boron has a high absorption cross section.

A high $\Delta k_{eff}$ indicates a large amount of neutrons being prevented from causing fission, meaning that boron has to absorb a lot of neutrons. As a large number of neutrons are absorbed in boron there will be a faster burnup of the boron. Therefore it can be concluded that where the multiplication of flux with adjoint is highest (largest $\Delta k_{eff}$) the burnup of a certain amount of boron will be highest.

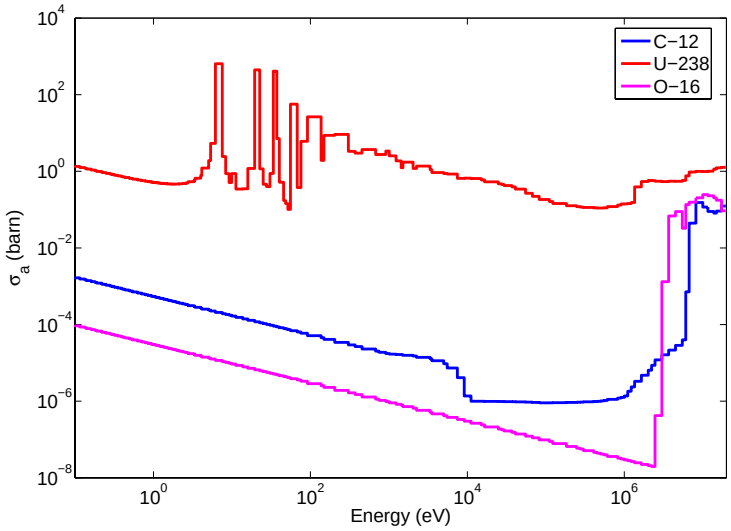


Figure 4.3: The microscopic cross sections ($\sigma_a$) for nuclides present in the U-Battery

## 4.3 Power peaking

Introducing boron into the reactor will change the burnup characteristics compared to a boron free reactor. The boron free reactor will have a power density distribution proportional to the flux times the macroscopic cross section for a certain location [Duderstadt and Hamilton, 1976]:

$$P''' = \int_E \Sigma_f(\mathbf{r}, E)\Phi(\mathbf{r}, E)E_{rel}dE \tag{4.8}$$

In this equation $E_{rel}$ is the energy released per fission. In reactor design it should be avoided to have too high local variations in the power density, because non homogeneous power distribution can cause high temperature differences between regions and with that high material stresses, causing material damages and failures. To measure the power distribution the power-peaking factor was introduced, which is defined as the peak-to-average power ratio

$$F_{pp} = \frac{P'''_{max}}{P'''_{ave}} \tag{4.9}$$

The maximum allowed value for the $F_{pp}$ for the U-Battery has not yet been determined. However a comparison can be made between the power-peaking factor for a borated and unborated core in order to determine whether boration deteriorates the power-peaking factor.

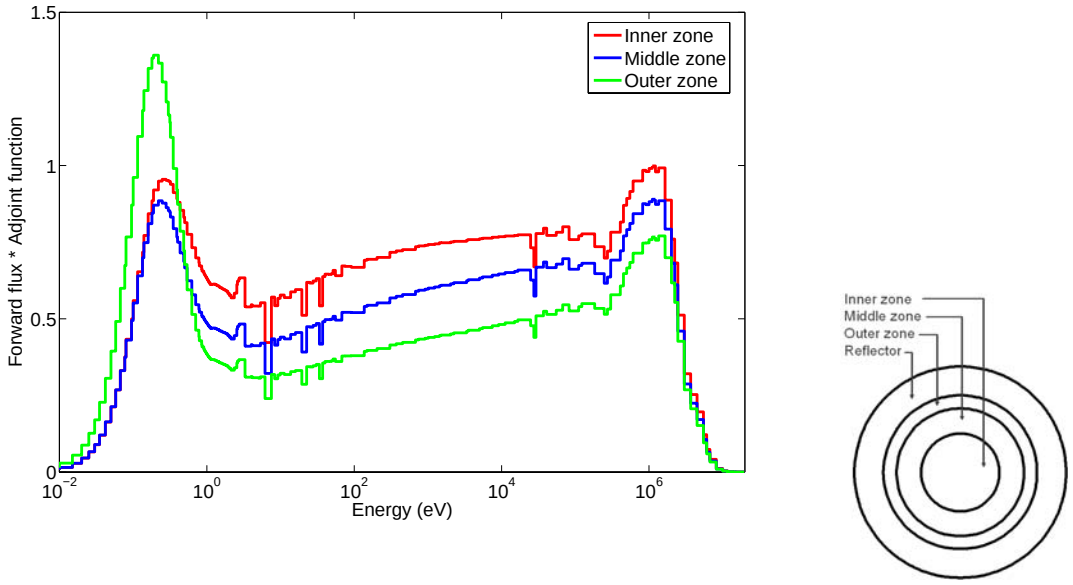


Figure 4.4: The adjoint function multiplied by the flux indicates the importance of zones on the $\Delta k_{eff}$

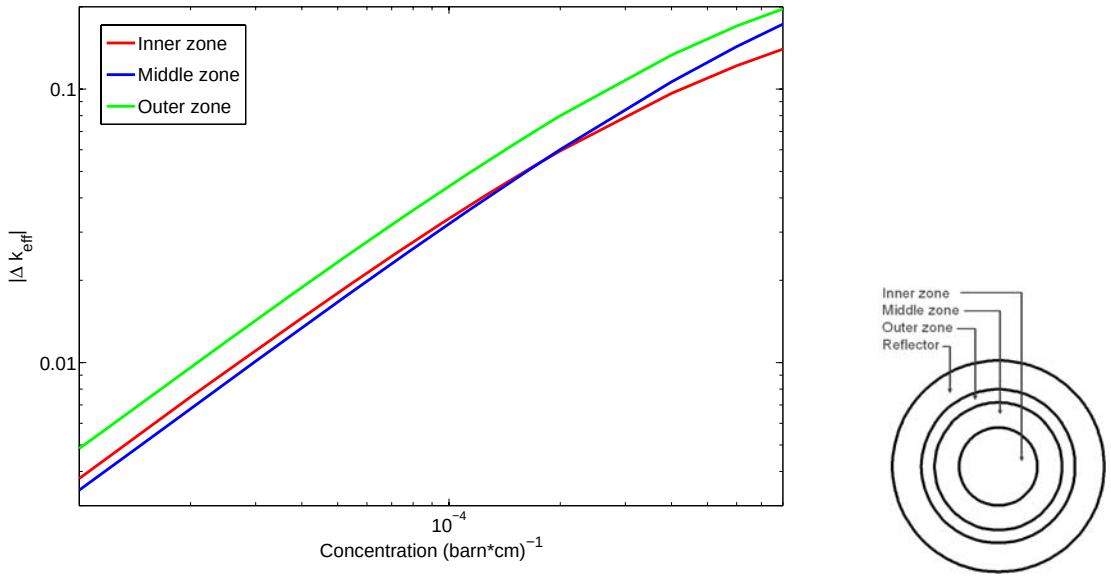


Figure 4.5: The influence of the insertion of boron on the $\Delta k_{eff}$. It can be seen that the influence scales with the product of the adjoint with the flux in the thermal region

# Chapter 5

# The U-battery

## 5.1 Reactor configuration

The U-battery is a small nuclear reactor design (5 to 10 $MW_e$) which can be operated for fuel cycles of 5 years and longer. The U-battery design is constrained by various parameters. These parameters are studied in an extensive study by De Zwaan [2007]. Choices made in this thesis concerning reactor configuration were based on that study. The moderator in the reactor is selected to be graphite. In addition to this choice several parameters influence the reactor configuration: Core power, fuel cycle period, burnup, initial fuel enrichment, fuel geometry and coolant.

Choices made for these parameters initiate new constraints on other parameters. The goal is to obtain an optimal configuration. Beside these free design parameters there is a hard constraint imposed on the design by the potential developers: The U-Battery has to be self regulating.

All choices made for the U-battery are summarised in table 5.1.

Table 5.1: Summary of the properties for the U-Battery modelled in this thesis

| Properties for the U-Battery | |
|---|---|
| Fuel | TRISO coated particles with $UO_2$ core |
| Coolant | $^7Li - Be$ fluoride salt(FLIBE) |
| Core Volume | $3m^3$ |
| Reflector | Graphite 60cm |
| Moderator | Graphite |
| FIMA | 10% |
| Power | 20 $MW_t$ |
| Zone radii from core centre | 62.0cm, 78.2cm and 89.5cm |
| Core temperature | 1073 °K |

By the use of the U-Battery a decentralised power supply becomes possible. This implicates that there will be no loss of energy by transportation through the power grid. Also this decentralisation mitigates against network failures as interruptions in the network are on a short distance line between plant and consumer and therefore easy traceable. There is a clear need for power which is not reliant on the commercial networks as large companies already have their own on-site power plant.

The U-Battery only needs one fuel batch every 5 or more years. This means owners of a U-Battery do not need a supply chain for fuel and fuel stockpile management to avoid power shortage. The price of energy will not be fluctuating during the lifetime of the U-Battery, which cannot be said of using fossil fuels.

The fuel chosen for the U-battery are TRISO coated fuel particles. These particles consist of uranium dioxide ($UO_2$) kernels with a diameter of half a millimetre. These uranium kernels are coated with several layers of pyrolytic carbon and silicon carbide. The SiC coating assures that the fission products are maintained inside the particle. The TRISO coated particle is able to stay intact and retain fission products up to 1600°C [Sterbentz et al., 2004]. A matrix fuel assembly was chosen to contain the TRISO particles.

The needed fuel inventory depends on the initial enrichment and the amount of thermal heat produced in the reactor core over the life-cycle. A combination of these values gives a certain burnup at the end of lifetime. The target burnup was set to 10% fission on initial metal atom (FIMA) as this percentage is easily reachable without significant increase of fuel failure [Gontard and Nabielek, 1990]. The nominal power of the U-Battery was set to 20 $MW_{th}$. As 5 years is the minimal fuel cycle length this is chosen as the initial fuel cycle length. The enrichment is set to 20%, the maximum allowable enrichment within non-proliferation treaties.

With the chosen fuel assembly the U-battery is set to maximum achievements, which keep options open to increase thermal power, lifetime or to lower enrichment.

There are several coolant candidates for the U-Battery: liquid metal (tin), helium, $CO_2$ and several liquid salts. The final choice for a coolant in this study was FLIBE a $^7Li - Be$ fluoride salt, although all mentioned coolants [De Zwaan, 2007] are still under consideration for the final version of the U-Battery. The choice of coolant is of very little influence on the problem in this thesis as the coolant does hardly absorb or moderate neutrons.

The size of the outer containment of the U-battery cannot be larger than $4.5m$ x $4.5m$ x $21m$ as this is the maximum allowable size for transportation by road. This limits the core size to $3.5m$ x $3.5m$ x $20m$ as half a meter is estimated to be needed on each side for housing and off-line shielding.

The neutron leakage has to be kept as low as possible since this will keep reactor lifetime as long as possible. Therefore the geometrical buckling needs to be minimised within the design constraints mentioned above. The geometrical buckling for a cylindrical core is minimised [Duderstadt and Hamilton, 1976] when the height, H and the diameter, D of the core relate to each other as

$$H = \frac{\pi\sqrt{2}}{2\nu_0} D = 0.924D \tag{5.1}$$

in which $\nu_0$ is 2.405... The factor $\nu_0$ is the first point where the zero order Bessel function describing the optimization problem [Duderstadt and Hamilton, 1976] is zero.

In order to be able to see if the approaches discussed in this report will work for different geometries there have been done calculations on a slightly different core design as well. This core is double in volume (6 $m^3$) and has a lower enrichment, 12%. The rest of the design is the same.

## 5.2 Modelling the U-battery

The U-battery is still a virtual design. Therefore several scripts have been written to model the reactor and its neutronic behaviour. Two different burnup scripts have been used in this thesis, KENOBURN and BURN1D. The principles of both scripts are the same. First the fuel geometry and composition are described in several zones as well as the power produced. With this reactor "mock-up" the cross sections as seen by a neutron are calculated. With the power a flux normalisation is determined. With the flux and new cross sections a depletion calculation is done, which is extrapolated to the number of burn days.

### 5.2.1 Geometrical modelling

The fuel mock-up determines the neutronic behaviour. This behaviour is averaged over the region in which the calculations are done. In this thesis different fuel mock-ups are needed for different regions in the reactor. Therefore the reactor is divided into several zones.

For KENOBURN the reactor has been divided into nine zones. Each zone has the same volume, so the distance between outer and inner radius is smaller for the outer zones than for the inner zones. The heights of all zones are equal. The different zones can be seen in figure 5.1a and the reference number of the zones in figure 5.1b.

The BURN1D code is one dimensional. Therefore the geometry was spherical and three radial zones were defined. These three zones have the same volume, so the difference between the outer and inner radii decrease going outwards from the midpoint. The radii

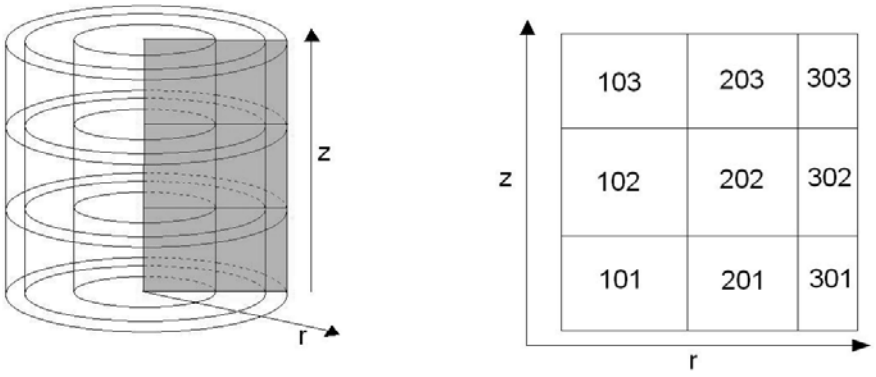


(a) Zones (b) Numbering of zones

Figure 5.1: The different zones used for the KENOBURN calculations and their reference numbering

are 62cm, 78cm and 89cm for zone 1, 2 and 3 respectively. The zone identifiers are shown in figure 5.2a.

The KENOBURN code is used to model the real properties of the U-Battery and to get an understanding of the processes in the reactor. However in the burnable poison calculations a lot of repeated calculations have to be done. Therefore BURN1D is used to model the U-Battery, as the calculation time for BURN1D is about one sixth of the calculation time for KENOBURN. The concepts derived in the 1-D model can then afterwards be implemented in the 2-D model with KENOBURN.

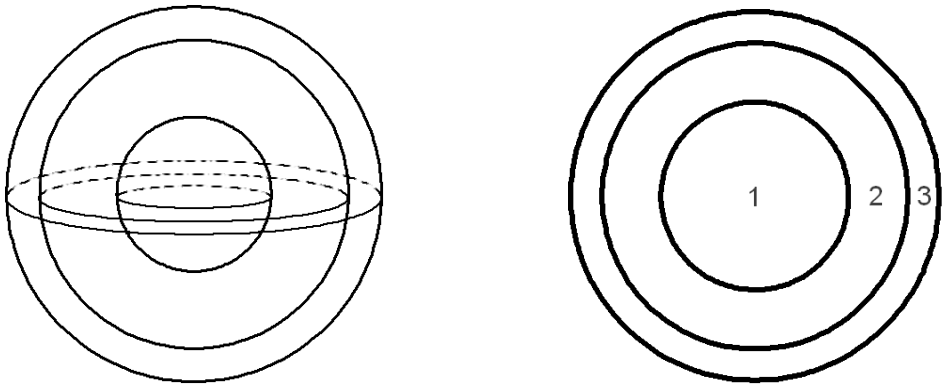


(a) Zones (b) Numbering of zones

Figure 5.2: Zones used in the BURN1D calculation

### 5.2.2 Burnup scripts

The programs BURN1D and KENOBURN are PERL scripts which couple the different SCALE 4.4 modules [ORNL, 2005]. It contains the input parameters, geometry and fuel, of the reactor. With this information it automatically creates input files for SCALE. The program flow is illustrated in figure 5.3. The difference between the programs is the number of dimensions it can handle. KENOBURN can handle 3 dimensions while BURN1D only can handle one dimension.

The first action taken in both burn scripts is to read the nuclides in the reactor core and reflector and the geometry of the reactor. From these data the CSASIX input is written and CSASIX is run. CSASIX is a criticality safety analysis sequence which includes XSDRNPM. CSASIX first runs BONAMI, then NITAWL, to create a working library with resonance shielded cross sections. With this working library it runs XSDRNPM, a transport code.The results of this XSDRNPM calculation are cell weighted cross sections for the different reactor zones with the same reaction rates as for the individual cells (fuel, cladding and moderator).

The cell weighted cross sections enter the first tier. The cross sections are entered into WAX. This module calculates the cross sections for the entire reactor by taking the cross sections for the reactor zones and to investigate the boundary conditions at the zone boundaries.

The output of WAX, the cell weighted cross sections [ORNL, 2005] for the entire reactor are entered into a new calculation. It is here where BURN1D and KENOBURN differ. In BURN1D a flux profile is calculated with XSDRNPM. XSDRNPM is only capable of solving 1-D problems so the output flux profile is 1-D. In KENOBURN however this flux profile is calculated with KENOV.a, which can handle 2-D and 3-D problems. Since the shape is a cylinder the flux profile is 2-D. The flux calculated in either of these SCALE modules is not yet normalised.

Normalisation is done by the non-SCALE program FLUX2POWER. This FORTRAN program reads the flux profile from the XSDRNPM calculation and normalises the flux towards the power given (P), by solving the equation

$$P = \int_V \int_E \Sigma_f(E) E_{rel}(E) \varphi(E) dE dV \tag{5.2}$$

in which $\Sigma_f$ is the macroscopic fission cross section, $E_{rel}(E)$ the power released per fission for energy value E and $\varphi(E)$ the flux per energy value E. The resulting normalised flux profile is the output and is given as input for the ORIGEN-S calculation. As well this XSDRNPM calculation gives a $k_{eff}$ for the reactor.

On the second tier the working library produced by NITAWL is taken and a zone weighted [ORNL, 2005] XSDRNPM cross section calculation is done. This gives the

cross sections weighted over the fuel, cladding and moderator. In COUPLE these nuclide cross sections are prepared for the ORIGEN-S depletion calculation.

In ORIGEN-S tier one and two come together. With the zone weighted cross sections for the fuel and the normalised flux the depletion calculation is done. Additional information needed for these calculations are the number of burnup days and cross sections for nuclides not in the original nuclide densities. These cross sections are generated by COUPLE from the master cross section library and have to be included as they give the properties for the fission products, which can influence the macroscopic cross sections. The ORIGEN-S depletion calculation gives new nuclide densities. These densities are entered for the calculation of the next time step.

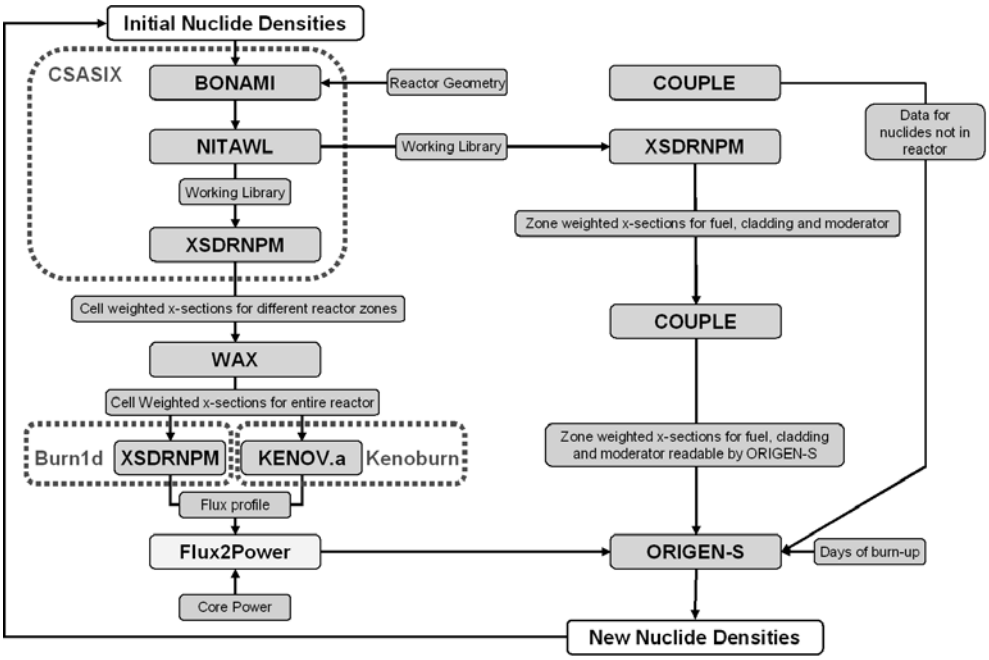


Figure 5.3: The calculation scheme used in the burnup programs BURN1D and KENOBURN

# Chapter 6

# Using adjoints in a reverse calculation

## 6.1 Approach

In section 4.2.3 it was shown that the boron burnup will be proportional to the adjoint function multiplied (in fact an inner product) by the neutron flux in the thermal region. Ideally all the boron has disappeared at the end of fuel lifetime, to avoid a shortening in lifetime. Therefore the idea is to distribute the boron in such a way that the boron atomic density is proportional to the product of the adjoint with the flux. This product does not take into account the energy dependence of the absorption by boron. In order to introduce this energy dependence the product is multiplied by the energy dependent absorption cross section of boron (figure 6.1). This is the energy dependence of $\alpha$ in equation 4.7. The values of this new product are used to determine the boron distribution used in the core. By collapsing[1] the outcome of the new product in energy, relative values for the three zones are obtained. The concentration distribution is described in table 6.1. This distribution will cause the most efficient burnup.

Table 6.1: The distribution of boron between the three zones based on the relative differences between $\langle \Phi\sigma_a, \Phi^* \rangle$

| | $\langle \Phi\sigma_a, \Phi^* \rangle$ | Percentage of boron |
|---|---|---|
| Inner zone | 3755 | 31% |
| Middle zone | 3394 | 28% |
| Outer zone | 4836 | 41% |

As the interrelation between the zones has now been fixed based on this assumption, equation 3.12 can be used to calculate the boron concentrations needed in each zone.

[1]The value calculated by collapsing does not indicate a usable quantity as the flux and adjoint used in the collapse have not been normalised yet.

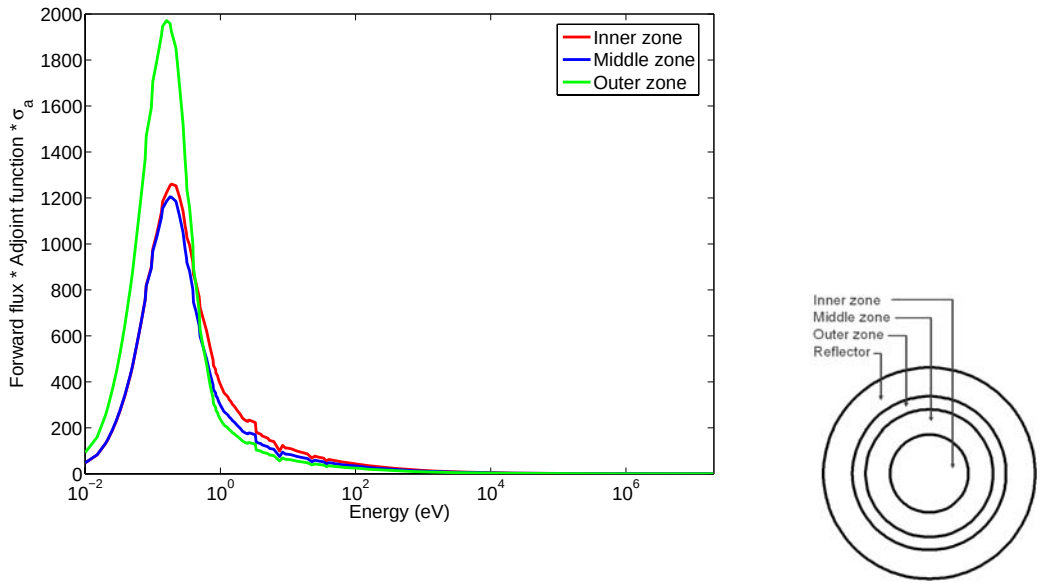


Figure 6.1: The multiplication of the flux with the adjoint and the microscopic absorption cross section of boron

The approach taken was first to do a burnup calculation with BURN1D (chapter 5) with time steps as shown in figure 6.2. Then from the end of the life cycle a step back in time is taken to an evaluated point in time (beginning of step 9). At this point the $\Delta\rho$ is evaluated, by determining the $k_{eff}$. When the $k_{eff}$ is outside the set boundaries (i.e. not between 0.99 and 1.01) there will be inserted some boron, according to the distribution as discussed above. Then the $k_{eff}$ will be checked again towards the boundaries. If it is still not between the boundaries the boron concentration will be adjusted. This process continues iteratively until the concentration is such that the $k_{eff}$ value is between the boundaries set. This implies that $\Delta\rho$ is zero and that the **M** operator, the absorption and scattering components, cancels the **F** operator, the fission component in equation 3.12. When the boron concentration is in between the boundaries a depletion calculation is done in order to see how much of the boron will be left for the next time step (end of step 9, beginning of step 10). Then a new step back in time is taken (to the beginning of step 8) and the process described above will be repeated for this time step. This process is repeated for each time step until the beginning of step 2. Step 1 is not evaluated since this step is the step in which the xenon and samarium poisoning occurs.

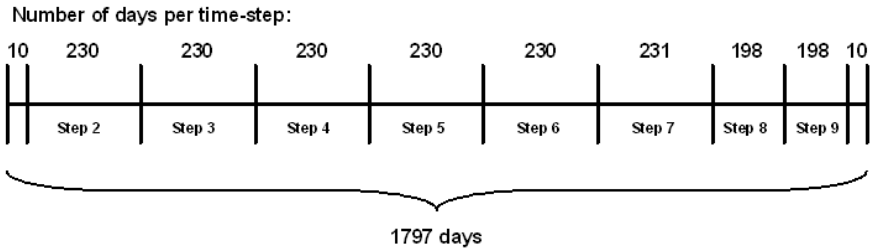


Figure 6.2: Time steps taken in the adjoint weigthed $^{10}$B calculations with the burnup time for each step in days

## 6.2 Results

The result of the calculations are shown in figure 6.3. The figure indicates at each time step (except the first) the amount of boron left after the depletion of the amount of boron in the previous step. As well at each time step the boron concentrations needed for a $k_{eff}$ of one are shown (except at the last time step). Because these concentrations are not the same, discontinuities can be seen in the figure. From this it can be concluded that the initial boron insertion in the first time step is depleted too fast to be able to compensate the over-reactivity at the end of the time step, the beginning of the next time step. The upward step at the discontinuity indicates that the zone should contain more boron at the end of the time step then is available after burnup. It can be seen that this is the case for each time step up until the step at around 1200 days. From this it can be concluded that an efficient burnup, boron distributed with the adjoint function multiplied with the flux, is unfavourable as the boron will deplete too fast throughout reactor life. The total system has to be able to "save" some boron for the later time steps in order to be able to compensate the reactivity.

After around 1200 days of burnup the boron does not deplete fast enough. At the end of the time steps there is still too much boron left, so the reactivity compensation is too high resulting in a $k_{eff}$ below 0.99. This will shorten the lifetime of the reactor, which is unwanted.

From the above it can be concluded that a boron distribution with the adjoint and flux multiplication is not a favourable configuration. A zone will have to be filled with more boron in order to save boron for next time steps, although it has to be burnt up enough to avoid the overcompensation in the end of lifetime. Another approach to the problem will be studied in chapter 7.

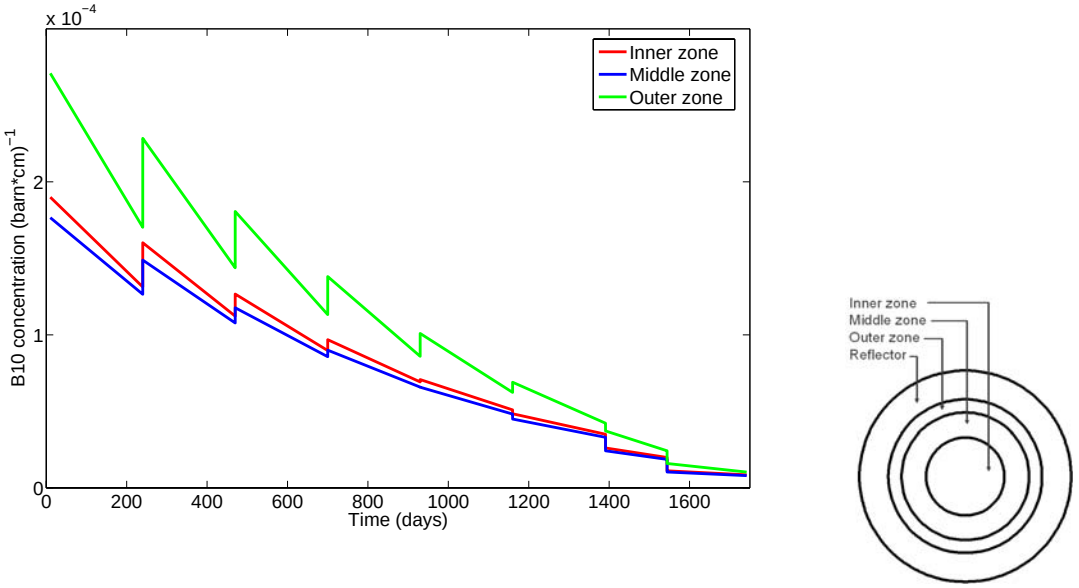


Figure 6.3: The adjoint weighted concentration $^{10}$B needed per zone for $k_{eff} = 1$ and the following burnup. The distribution of the boron concentrations is relative to the product of the adjoint function with the flux and the absorption cross section of boron.

# Chapter 7

# Parameter study

As described in the previous chapter a new approach has to be used to determine the optimal boron distribution. Therefore a parameter study was done. This parameter study was first conducted in a two variable model (the boron atomic densities in two zones) and later in a three variable model (the boron atomic densities in three zones). This was done to save computing time. Computing time, keeping the same resolution, goes up exponentially with the number of variables. As well it might be possible to find a solution to the problem by only varying two variables, making a calculation with more variables unnecessary as the reactor should be kept as simple as possible.

## 7.1 Two variable parameter approach

### 7.1.1 Initial calculations

In this approach the independent variables are the atomic densities of boron in two zones. Each combination of zones was studied and the zones used are the zones indicated in figure 5.2a. The boron concentration in the remaining, third zone is kept constant at zero. The boron densities in the two varying zones are given each a value between zero and $1.10^{-3}$ with a step-size of $1.10^{-4}$ . A combination of densities in this order of magnitude will be able to compensate the total over-reactivity present, as can be seen in figure 4.5.

For each combination of these variables, the boron atomic density in each of the two zones, a burnup calculation was done with the burnup times as shown in figure 7.1. At each of these points in time a $k_{eff}$ evaluation was done, except at the beginning of reactor life. This because the $k_{eff}$ at this point will be high due to the absence of samarium and xenon poisoning. The evaluation of the $k_{eff}$ consisted of determining the deviation of the $k_{eff} = 1$ line. The absolute maximum deviation, $\Delta k$, is the parameter influenced by the variables, that needs to be minimised, as this is the maximum reactivity swing that should be within the boundaries as described in section 2.3.

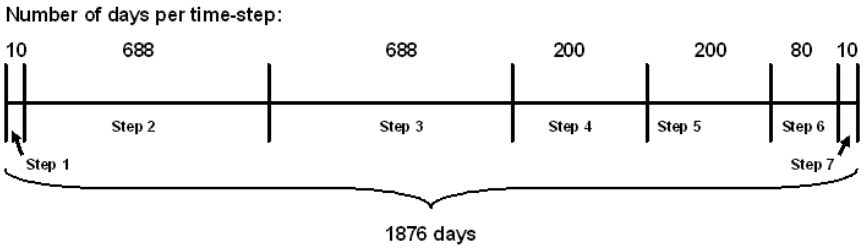


Figure 7.1: The burnup times used for the different time steps in the parameter study

A second parameter calculated was the shortening of fuel lifetime. This was done by first determining the lifetime of a reactor without poison. Linear interpolation between the value for which the $k_{eff}$ is still above 0.99 and the first value for which $k_{eff}$ is below 0.99 was used to determine the lifetime. The reactor lifetime with no poison, calculated with this method was 1856 days. Then for each combination of densities, by a similar interpolation method, the lifetime was determined. By subtracting this from the lifetime of the poison free reactor the shortening of lifetime, $\Delta t$, was obtained.

The two parameters obtained, the absolute maximum deviation from $k_{eff} = 1$ and the shortening in lifetime are plotted as contour plots.

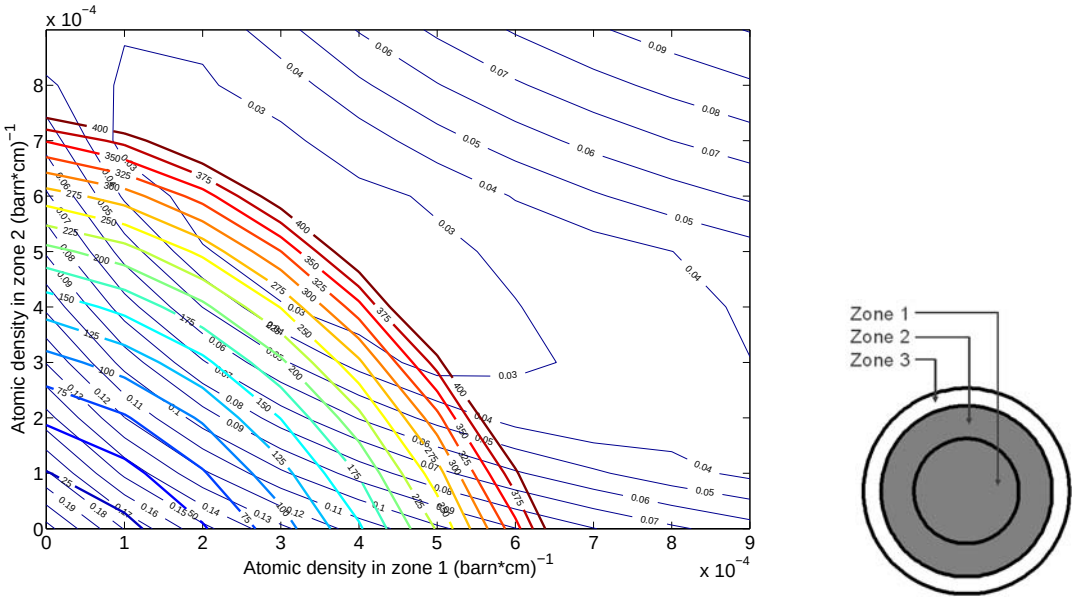


Figure 7.2: The maximum deviation from the line $k_{eff} = 1$ is shown in the slim blue lines ($\Delta k$), while the shortening in lifetime (in days) is shown in the coloured bold lines ($\Delta t$), for the boron atomic density in zone 1 and 2 as variables

In figure 7.2 the shortening in lifetime and the deviation from the $k_{eff} = 1$ line is shown when the boron atomic densities in zone 1 and 2 are varied. When, for example, a boron density of $2.10^{-4}$ in zone 1 and a density of $3.10^{-4}$ in zone 2 is taken, it can be seen from the figure that the maximum deviation from the line $k_{eff} = 1$ is between 0.07 and 0.08. This can be concluded as the point is between the slim blue lines indicating a deviation of 0.07 and 0.08. The shortening in lifetime for these densities is between 125 and 150 days, since the point is between the bold coloured lines indicating 125 and 150 days loss of lifetime.

The figure shows a trend of decreasing deviation from the line $k_{eff} = 1$ with increasing boron density in zone 1 while keeping the density in zone 2 constant. The deviation however starts to increase again when a certain minimum is passed. This decreasing deviation, passing a minimum and then increasing deviation can be seen as well when varying the boron density in zone 2 and keeping the density in zone 1 constant. However the change in deviation is faster when the density in zone 2 is varied. The shortening in lifetime increases with the boron density in zone 1 and 2 as well, although the shortening increases fastest by increasing the boron density in zone 1.

It can be seen from figure 7.2 that the lowest reactivity swing is below 3%. For this swing the shortening in lifetime is more than 250 days.

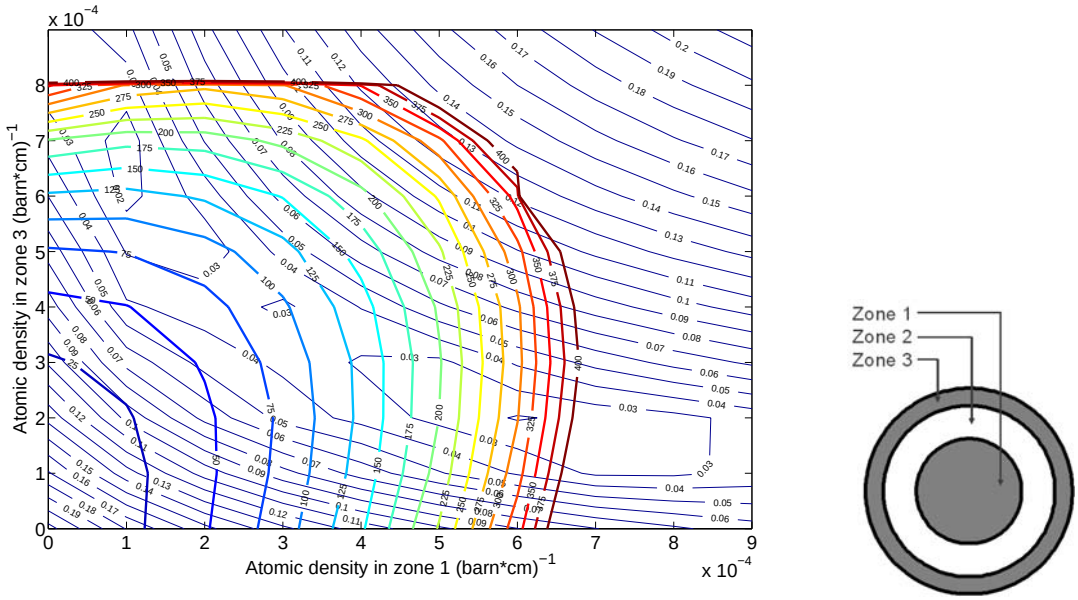


Figure 7.3: The maximum deviation from the line $k_{eff} = 1$ is shown in the slim blue lines ($\Delta$k), while the shortening in lifetime (in days) is shown in the coloured bold lines ($\Delta$t), for the boron atomic density in zone 1 and 3 as variables

In figure 7.3 the shortening in lifetime and the deviation from the $k_{eff} = 1$ line is shown when the varied values are the atomic densities in zone 1 and 3. It can be seen that there are two "regions" in which the reactivity swing is as low as 2%. From the graph it can be seen that one of these "regions", the "region" with an atomic density between $6.10^{-4}$ and $7.10^{-4}$ in zone 3 and an atomic density of around $1.10^{-4}$ in zone 1 has a shortening in lifetime between 100 and 225 days. The other "region" with a swing of around 2%, the region around the densities $2.10^{-4}$ and $6.10^{-4}$ in zones 3 and 1 respectively, has a shortening of lifetime of around 300 days. The former "region" is therefore more favourable as a solution.

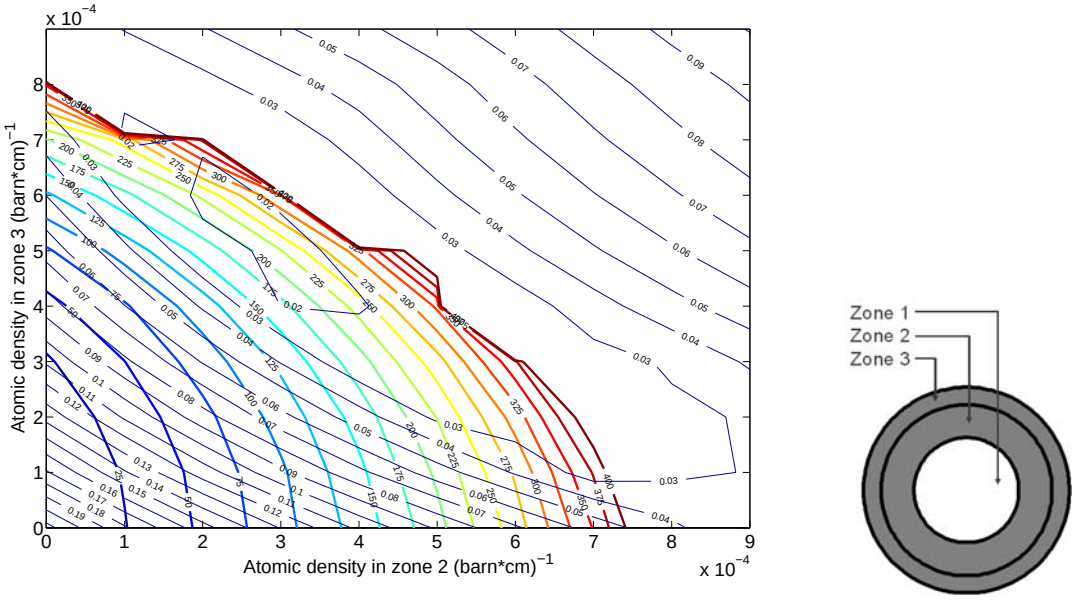


Figure 7.4: The maximum deviation from the line $k_{eff} = 1$ is shown in the slim blue lines ($\Delta$k), while the shortening in lifetime (in days) is shown in the coloured bold lines ($\Delta$t), for the boron atomic density in zone 2 and 3 as variables

In figure 7.4 the shortening in lifetime and the deviation from the $k_{eff} = 1$ line is shown when the varied values are the atomic densities in zone 2 and 3. The lowest reactivity swing is around 2 %. However when the swing is at this low point the number of days lost is between 175 and 350 days. This is due to the steep increase of shortening of fuel lifetime with the increase in boron densities in zone 2 and 3.

Comparing the three graphs with each other it can be seen that the most favourable configuration is a combination of high boron density in the outer zone (zone 3) and a low density in the inner zone (zone 1). This complies with the theory that a high poison density is favourable in the zone where the adjoint function times the flux is high (in the thermal region) and then a poison presence is favourable in the zone where this

multiplication is second highest. This theory was developed in subsection 6. The zone with the highest product of flux and adjoint function needs more poison to be able to "save" reactivity compensation throughout the lifetime of the reactor.

### 7.1.2 Expansion of the two variables

The calculations with two zones limits the spatial configuration. With these two variables a reactivity swing below 1% can not be achieved. In order to reduce the reactivity swing even more, the concentration distribution with the lowest deviation from the $k_{eff} = 1$ line is taken as a starting point. This point is the point with the atomic densities of $1.10^{-4}$ and $7.10^{-4}$ in zone 1 and 3 respectively (figure 7.3). The total amount of poison present is supposed sufficient to compensate for the entire reactivity swing for the entire reactor as the swing is already quite low and there is poison left causing the shortening in lifetime.

The approach is to split each of the three zones, as shown in figure 5.2b, into two separate zones of equal volume, creating a total reactor configuration of six zones, with equal volume, as shown in figure 7.5. The average poison density in zone a and b (the former zone 1) is kept equal to the former zone 1. This is done as well for zone e and f (the former zone 3).[1] Keeping the average densities constant (over former zone 1 and 3), the distribution between zone a and b and between e and f are changed and burnup calculations are done, to see if a more favourable configuration can be achieved.

The results of these calculations are shown in figure 7.6. In this figure only the 14

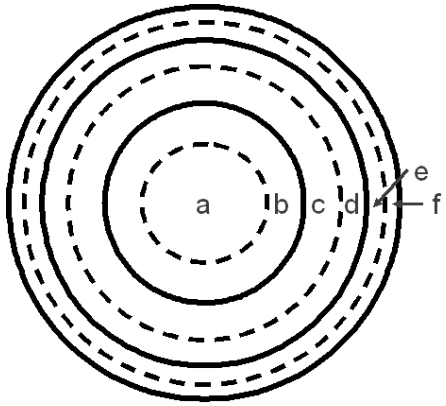


Figure 7.5: The six zones used in the expansion of the two and three parameter approach. All zones have the same volume.

lowest reactivity swings are plotted as well as the original situation from the two zone calculation. It can be seen that the configuration for the lowest swings favours a high density in the outer zone f and only a small density in zone e. This concurs with the theory developed in subsection 6, but again needing an above proportional amount in the

[1] Although zone 2 is split as well, this degree of freedom is not used here. This particular splitting is done to facilitate future calculations with three parameters

zone with the highest multiplication of the adjoint with the flux in the thermal region. The lowest swing obtained is a swing of around 1.3%, which still is not lower than the wanted 1%.

## 7.2 Three variable parameter approach

In the previous section an approach was chosen by varying two of the three atomic densities for the three zone configuration (figure 5.2b). This was done to keep calculation time as short as possible. In this section a three variable approach will be used with a slightly different approach in order to keep the calculation time in this configuration as low as possible.

### 7.2.1 Initial calculations

In this model a three variable approach was taken. Each of the densities in zone 1, 2 and 3 (figure 5.2b) are changed independently. Each of the densities is varied between $1.10^{-4}$ (zero has already been evaluated in the two parameter study) and $7.10^{-4}$ with an increase of $2.10^{-4}$. This was done at a coarse mesh to save computing time.

For each point evaluated in the calculations the absolute maximum deviation from the $k_{eff} = 1$ line was calculated as well as the lifetime shortening. The results are shown in table 7.1. This table shows the ten points with the lowest reactivity swing, sorted in descending order. As can be seen the lowest deviation and shortening in lifetime is found for the atomic densities of $1.10^{-4}$, $1.10^{-4}$ and $5.10^{-4}$ in zones 1, 2 and 3 respectively.

Table 7.1: The atomic densities for which the ten smallest absolute deviations from the line $k_{eff} = 1$ are calculated ($\Delta k$) and their shortening in lifetime in days ($\Delta t$).

| Atomic Densities | | | Parameters | |
|---|---|---|---|---|
| Zone 1 | Zone 2 | Zone 3 | $\Delta k$ | $\Delta t$ |
| 0.0001 | 0.0001 | 0.0005 | 0.0209 | 109 |
| 0.0001 | 0.0007 | 0.0001 | 0.0222 | 402 |
| 0.0005 | 0.0003 | 0.0001 | 0.0225 | 363 |
| 0.0005 | 0.0001 | 0.0001 | 0.0249 | 247 |
| 0.0007 | 0.0001 | 0.0001 | 0.0249 | 552 |
| 0.0001 | 0.0003 | 0.0003 | 0.0271 | 140 |
| 0.0001 | 0.0005 | 0.0001 | 0.0282 | 222 |
| 0.0003 | 0.0003 | 0.0001 | 0.0286 | 189 |
| 0.0003 | 0.0005 | 0.0001 | 0.0294 | 319 |
| 0.0003 | 0.0001 | 0.0003 | 0.0301 | 113 |

As the calculated grid has a low resolution a new grid was created around the point with the lowest deviation from the $k_{eff} = 1$ line. This grid runs from $5.10^{-5}$ to $1.5.10^{-4}$ in

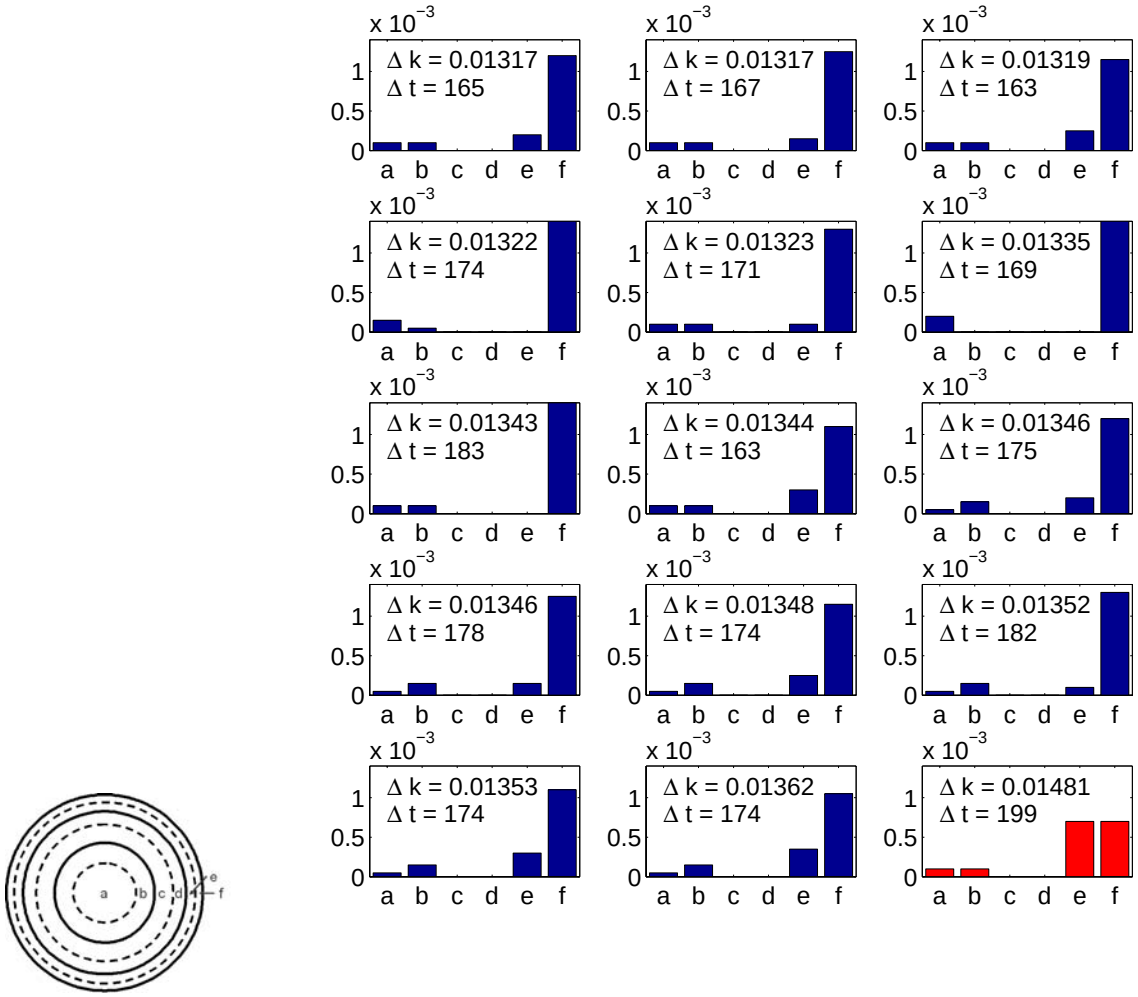


Figure 7.6: Atomic densities of boron, in $(\text{barn} * \text{cm})^{-1}$ on the vertical axes, in the zones a to f sorted by $\Delta$k in ascending order. The lower right picture with the red bars shows the two zone configuration which had the lowest reactivity swing. High densities in the outer region f in combination with low densities in the inner zones give rise to the lowest $\Delta$k

Table 7.2: The atomic densities for which the ten smallest absolute deviations from the line $k_{eff} = 1$ are calculated ($\Delta k$) and their shortening in lifetime in days ($\Delta t$) for a higher resolution around the lowest value in table 7.1

| Atomic Densities | | | Parameters | |
|---|---|---|---|---|
| Zone 1 | Zone 2 | Zone 3 | $\Delta k$ | $\Delta t$ |
| 1.00E-04 | 5.00E-05 | 6.00E-04 | 0.0126 | 134 |
| 5.00E-05 | 1.50E-04 | 5.50E-04 | 0.0134 | 155 |
| 5.00E-05 | 1.00E-04 | 6.00E-04 | 0.0135 | 161 |
| 5.00E-05 | 5.00E-05 | 6.00E-04 | 0.0137 | 137 |
| 5.00E-05 | 1.50E-04 | 6.00E-04 | 0.0143 | 186 |
| 1.00E-04 | 1.00E-04 | 5.50E-04 | 0.0147 | 130 |
| 5.00E-05 | 1.00E-04 | 5.50E-04 | 0.0159 | 131 |
| 1.00E-04 | 1.50E-04 | 5.00E-04 | 0.0168 | 129 |
| 5.00E-05 | 1.50E-04 | 5.00E-04 | 0.0180 | 129 |
| 1.00E-04 | 5.00E-05 | 5.50E-04 | 0.0189 | 111 |

steps of $5.10^{-5}$ for the atomic density in zones 1 and 2. Zone 3 has densities ranging from $4.5.10^{-4}$ to $6.10^{-4}$ in steps of $5.10^{-5}$. Again for each combination of densities a burnup calculation was done and the absolute deviation of the $k_{eff} = 1$ line evaluated as well as the shortening in lifetime. These results are shown in table 7.2. From the table it can be seen that the lowest reactivity swing is with boron densities of $1.10^{-4}$, $5.10^{-5}$ and $6.10^{-4}$ in zones 1, 2 and 3 respectively.

### 7.2.2 Expansion of the three variables

As a reactivity swing below 1% cannot be achieved using only three spatial zones, again an expansion of the approach is needed. Again the distribution with the lowest $\Delta k$ is chosen as a staring point. The initial three zones are divided into six zones with equal volume (figure 7.5). The total amount of poison is, just as in the two zone expansion (subsection 7.1.2), supposed to be sufficient to compensate for the entire reactivity swing. Average poison densities over former zones (figure 5.2b) is kept constant and only varied in distribution between the two new zones (figure 7.5) into which the old zones were split.

The results of these calculations are shown in table 7.3 and figure 7.7. It can be seen that there are several configurations for which the reactivity swing is below 1%. The lowest swing is realised with densities $5.10^{-5}$, $5.10^{-5}$, $2.5.10^{-5}$, $7.5.10^{-5}$, $4.10^{-4}$ and $8.10^{-4}$ in zone 1,2,3,4,5 and 6 respectively. With this configuration the number of days lost, $\Delta t$, is 139. Again it can be seen that a high density in the outer zone f is favourable.

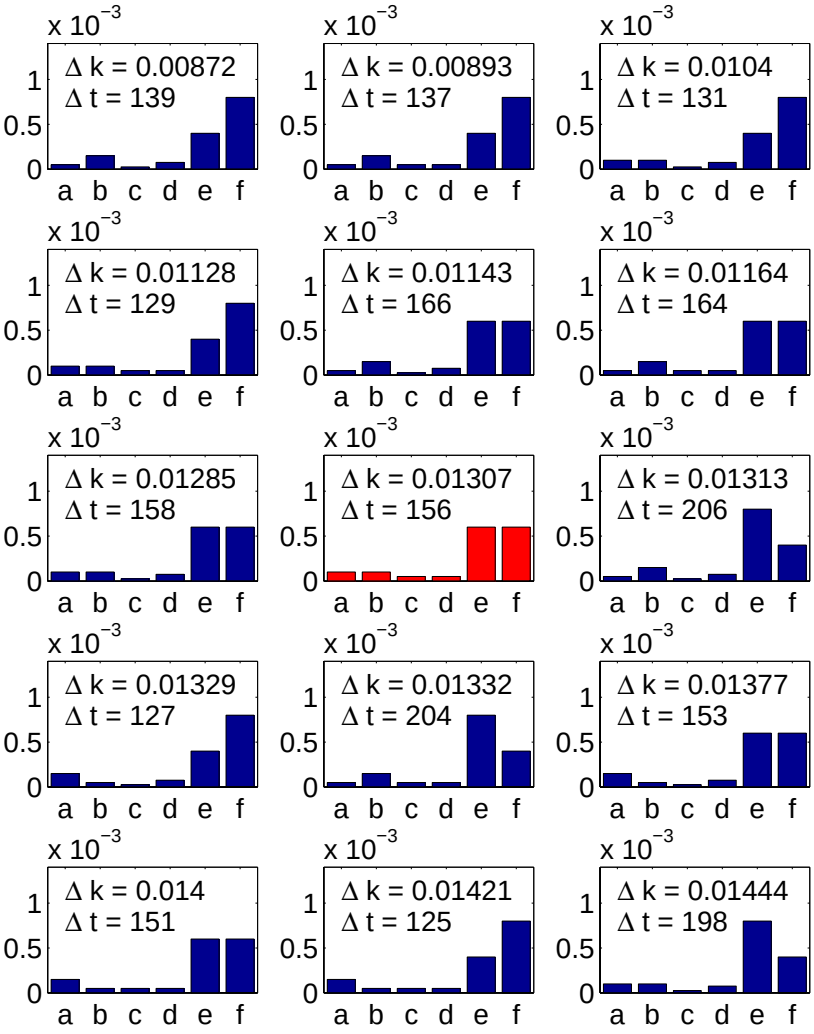


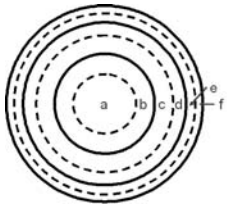


Figure 7.7: Atomic densities of boron, in $(\text{barn} * \text{cm})^{-1}$ on the vertical axes, in the zones a to f sorted by $\Delta$k in ascending order. The central picture with the red bars shows the optimal three zone configuration. A high density in the outer zone f is favoured for a low $\Delta$k

Table 7.3: The atomic densities for which the fifteen smallest absolute deviations from the line $k_{eff} = 1$ are calculated ($\Delta k$) and their shortening in lifetime in days ($\Delta t$), when a six zone calculation is conducted.

| Atomic Densities | | | | | | Parameters | |
|---|---|---|---|---|---|---|---|
| Zone a | Zone b | Zone c | Zone d | Zone e | Zone f | $\Delta k$ | $\Delta t$ |
| 0.00005 | 0.00015 | 0.000025 | 0.000075 | 0.00040 | 0.00080 | 0.00872 | 139 |
| 0.00005 | 0.00015 | 0.000050 | 0.000050 | 0.00040 | 0.00080 | 0.00893 | 137 |
| 0.00010 | 0.00010 | 0.000025 | 0.000075 | 0.00040 | 0.00080 | 0.01040 | 131 |
| 0.00010 | 0.00010 | 0.000050 | 0.000050 | 0.00040 | 0.00080 | 0.01128 | 129 |
| 0.00005 | 0.00015 | 0.000025 | 0.000075 | 0.00060 | 0.00060 | 0.01143 | 166 |
| 0.00005 | 0.00015 | 0.000050 | 0.000050 | 0.00060 | 0.00060 | 0.01164 | 164 |
| 0.00010 | 0.00010 | 0.000025 | 0.000075 | 0.00060 | 0.00060 | 0.01285 | 158 |
| 0.00010 | 0.00010 | 0.000050 | 0.000050 | 0.00060 | 0.00060 | 0.01307 | 156 |
| 0.00005 | 0.00015 | 0.000025 | 0.000075 | 0.00080 | 0.00040 | 0.01313 | 206 |
| 0.00015 | 0.00005 | 0.000025 | 0.000075 | 0.00040 | 0.00080 | 0.01329 | 127 |
| 0.00005 | 0.00015 | 0.000050 | 0.000050 | 0.00080 | 0.00040 | 0.01332 | 204 |
| 0.00015 | 0.00005 | 0.000025 | 0.000075 | 0.00060 | 0.00060 | 0.01377 | 153 |
| 0.00015 | 0.00005 | 0.000050 | 0.000050 | 0.00060 | 0.00060 | 0.01400 | 151 |
| 0.00015 | 0.00005 | 0.000050 | 0.000050 | 0.00040 | 0.00080 | 0.01421 | 125 |
| 0.00010 | 0.00010 | 0.000025 | 0.000075 | 0.00080 | 0.00040 | 0.01444 | 198 |

## 7.3 Large core calculations

The large core calculations have been done to confirm the methodology developed in the previous sections of this chapter. A core with other properties (described in the end of section 5.1) than the core in previous calculations was used. The difference in the properties between the previously used core and the large core are the volume ($6m^3$) and the enrichment (12%). The calculation method is the same: a 1-D calculation with BURN1D. As at this point it was known that zones 1 and 3 would give the best results, these zones were selected as the zones in which the boron atomic density would be varied. The results of initial calculations at a coarse mesh are shown in figure 7.8. There is no "region" with a $\Delta k$ of less than 0.02. However it can be seen that the region with high densities in zone 3 and low densities in zone 1 is unresolved. For example the point with atomic densities of $1.10^{-4}$ and $11.10^{-4}$ for zones 1 and 3 respectively is between two lines with equal $\Delta k$ of 0.095 without being enclosed.

A finer mesh was created in the region between atomic densities of $1.10^{-4}$ and $3.10^{-4}$ for zone 1 and atomic densities of $6.10^{-4}$ and $14.10^{-4}$ for zone 3 as this region did not show a clear behaviour. The result of this finer mesh is shown in figure 7.9. It turns out that the lowest $\Delta k$ is found for atomic densities of $1.10^{-4}$ and $13.10^{-4}$ for zone 1 and 3 respectively.

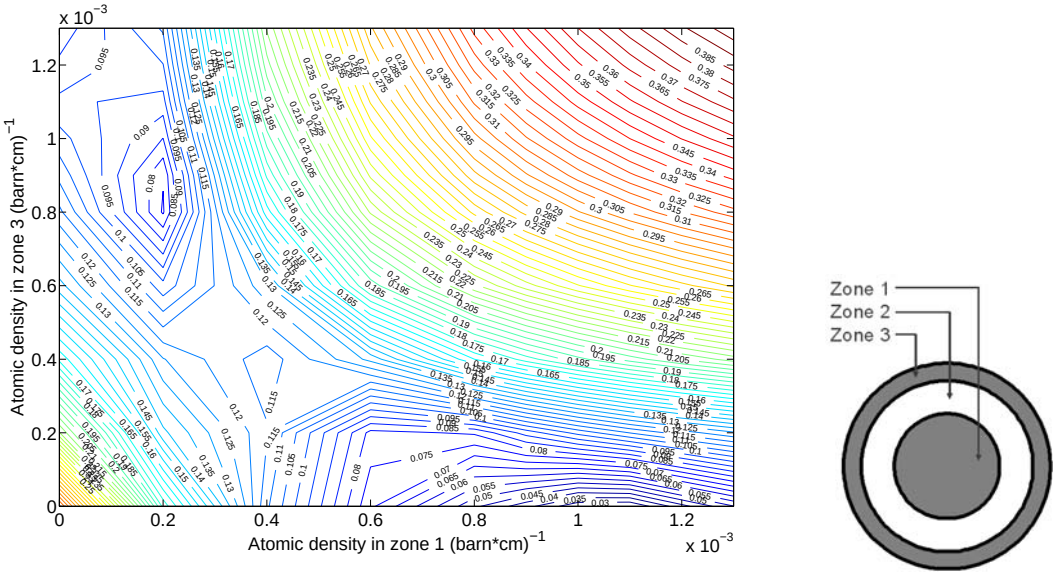


Figure 7.8: The maximum deviation from the line $k_{eff} = 1$ when the values for the atomic densities in zone 1 and 3 have been varied in a coarse mesh. A large core of 6 $m^3$ with 12% enrichment has been used. The region for large densities in zone 3 and low densities in zone 1 is unresolved and a finer mesh was created in figure 7.9

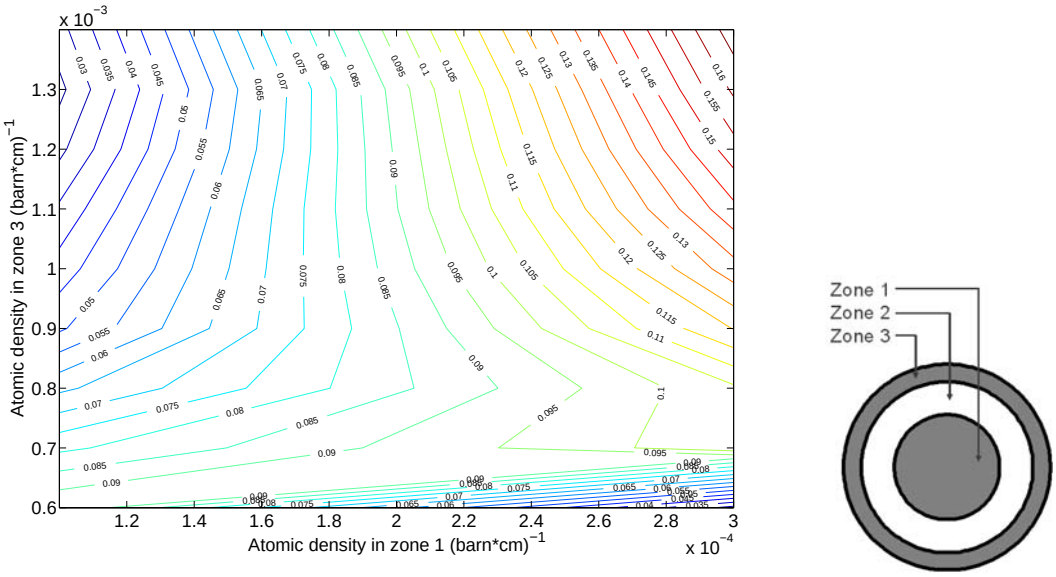


Figure 7.9: The maximum deviation from the line $k_{eff} = 1$ when the values for the atomic densities in zone 1 and 3 have been varied in a fine mesh. A large core of 6 $m^3$ with 12% enrichment has been used

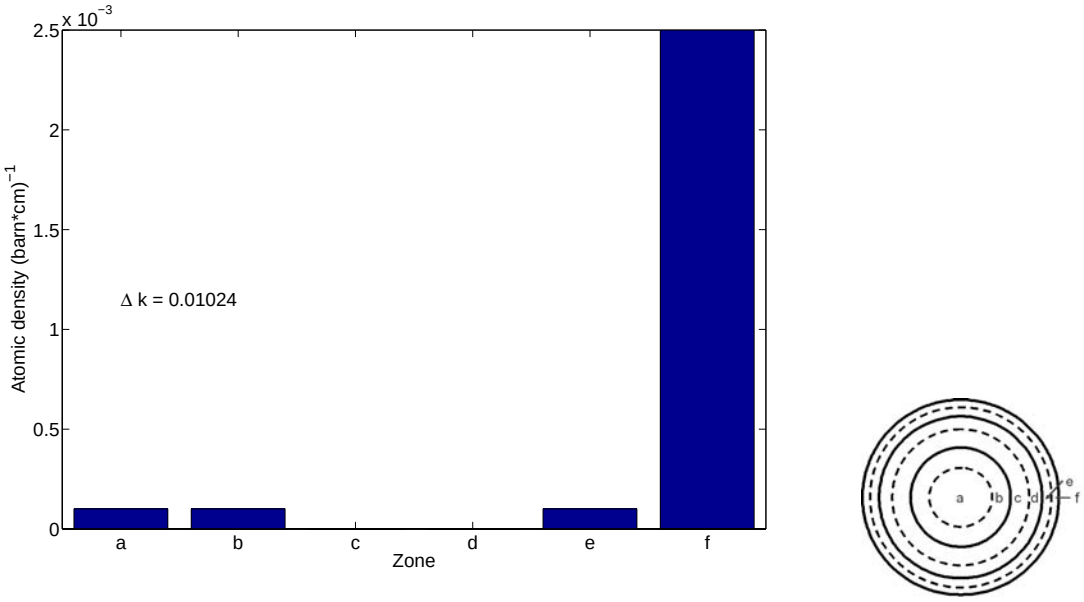


Figure 7.10: Atomic densities of boron in the zones a to f which yields the lowest $\Delta$k from the line $k_{eff} = 1$ for a large core of 6 $m^3$ with 12% enrichment

This value is taken as a starting point for the expansion of zones just as described in subsection 7.1.2. The result which yielded the lowest $\Delta$k of 0.0124, is shown in figure 7.10. This was the case for atomic densities of $1.10^{-4}$ in zones a, b and e and a density of $25.10^{-4}$ in zone f. In the large core calculations there was no shortening in fuel lifetime and even a small increase in fuel lifetime. This small increase in fuel lifetime can be contributed to a more favourable distribution of burnup.

## 7.4 Reflector poisoning

Due to the fact that a high boron density is favoured in the outer reactor region, this indicates, that a boron insertion into the reflector might be favourable. Although it is yet still unknown whether boron insertion is feasible, as discussed in chapter 1, an attempt has been made in order to establish thoughts on boron insertion into the reflector.

The analysis has been done by introducing boron into a zone in the reflector with a radius just as wide as the outer zone in the three zone model. As the burnup script cannot handle the burnup of non-fuel zones, the reflector with boron was modelled as a fuel zone with an uranium atomic density about 100 times smaller than in the real fuel zones. This was done to minimise the extra reactivity introduced in the reactor. Zone 1 and 3 were chosen as a second zone for boron insertion as the zone 1 and 3 combination gave the best results in previous calculations.

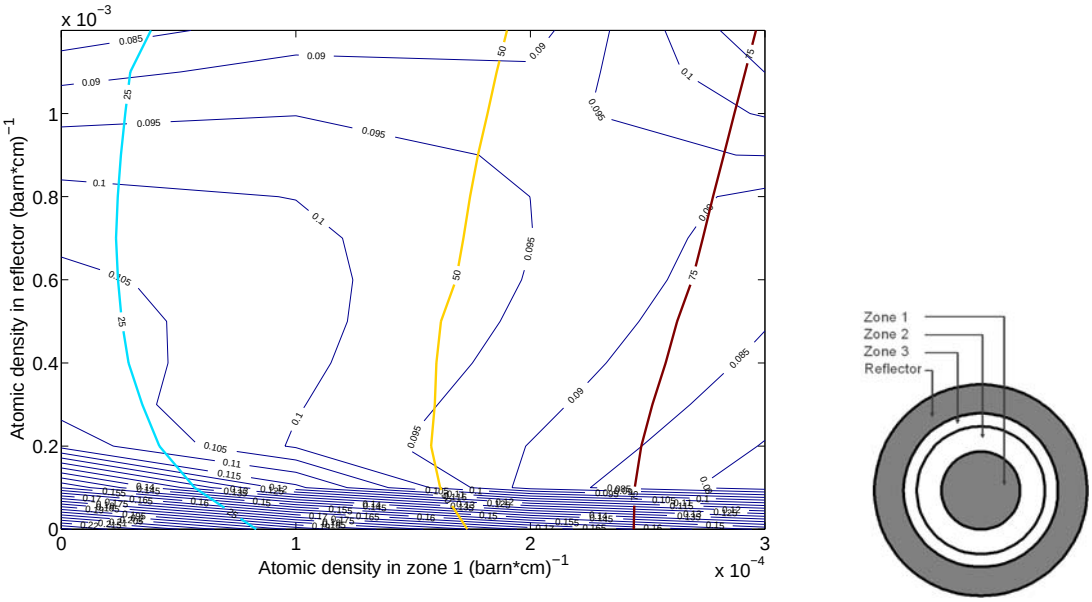


Figure 7.11: The maximum deviation from the line $k_{eff} = 1$ is shown in the slim blue lines ($\Delta$k), while the shortening in lifetime (in days) is shown in the coloured bold lines ($\Delta$t), for the boron atomic density in zone 1 and the reflector as variables

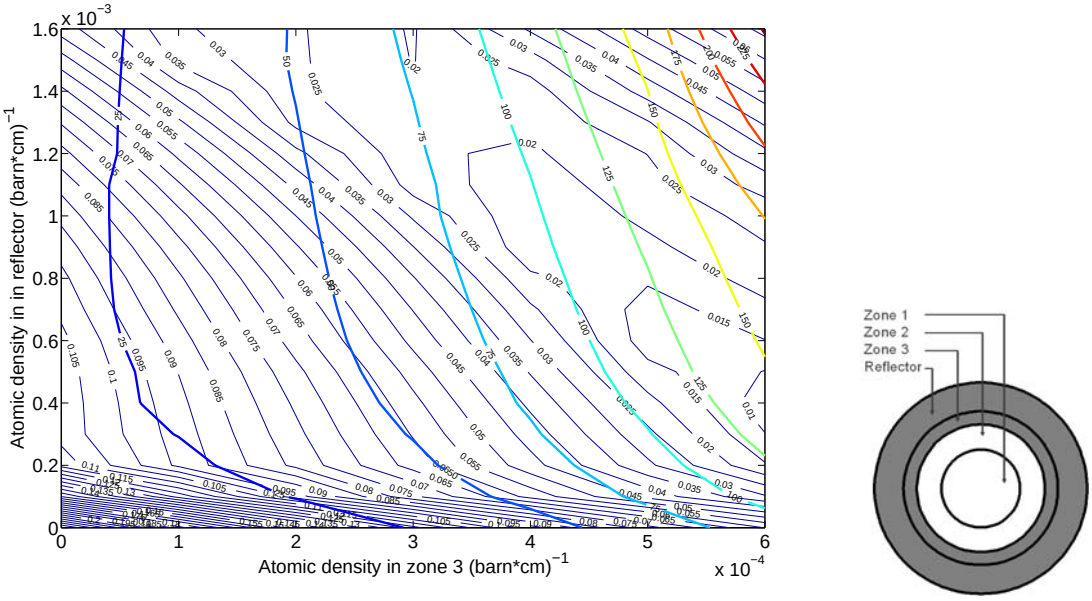


Figure 7.12: The maximum deviation from the line $k_{eff} = 1$ is shown in the slim blue lines ($\Delta$k), while the shortening in lifetime (in days) is shown in the coloured bold lines ($\Delta$t), for the boron atomic density in zone 3 and the reflector as variables

The results of these calculations are shown in figure 7.11 for zone 1 and in figure 7.12 for zone 3. When boron was inserted in the reflector and zone 1 a large minimum reactivity swing can be seen of around 8%. This swing is found in the region when there is more poison in zone 1 than in the reflector. When the density in zone 3 is varied it can be seen that a reactivity swing as low as 1% can be reached. This low swing however shows that a higher density of boron is favoured in zone 3 than in the reflector. The shortening in fuel lifetime in this case is between 125 and 150 days.

From both figures (7.11 and 7.12) it can be seen that an initial small insertion of boron in the reflector yields a rapid decrease of the $\Delta$k since there is a steep change in $\Delta$k between a boron atomic density of 0 and $1.10^{-4}$ in the reflector (the iso-$\Delta$k lines are close together).

## 7.5 Power peaking

As discussed in section 4.3, a comparison of the power densities can be made between the borated and unborated core to determine if there is an improvement in peak-to-average factor (equation 4.9). This factor was evaluated at beginning of fuel lifetime (BOL) and at the end of fuel lifetime (EOL). The average power density is calculated as the total power, 20 $MW_{th}$, divided by the core volume, $3m^3$. The average value is 6.66 $W/cm^3$. In figure 7.13 the power density distribution for the core is shown for an unborated and a borated core at BOL. When the peaks are taken for both curves a peak-to-average power ratio can be calculated. These are 1.81 and 1.61 for the unborated and borated core respectively.

In figure 7.14 the power density distribution for the core is shown for an unborated and a borated core at EOL. Both curves resemble each other close, although there is a slightly higher power density near the core edge for the borated core. At the peaks the calculated peak-to-average power ratio are 2.08 and 2.10 for the unborated and borated core respectively.

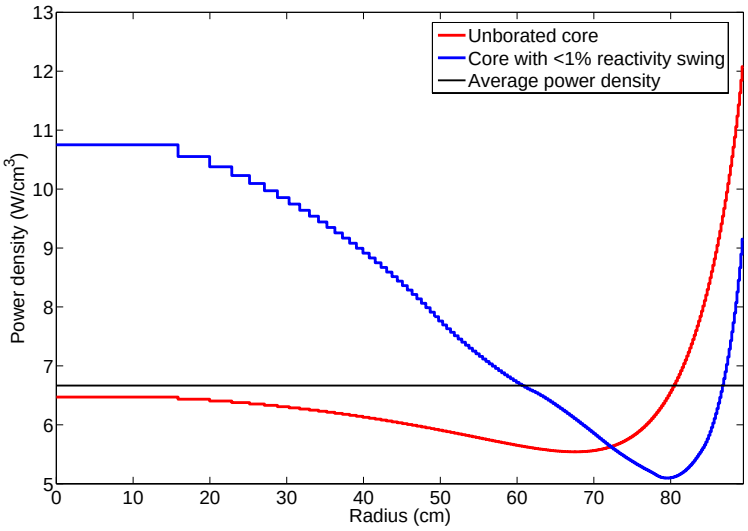


Figure 7.13: The power density in the radial direction for an unborated core and a core with less than 1% reactivity swing at BOL

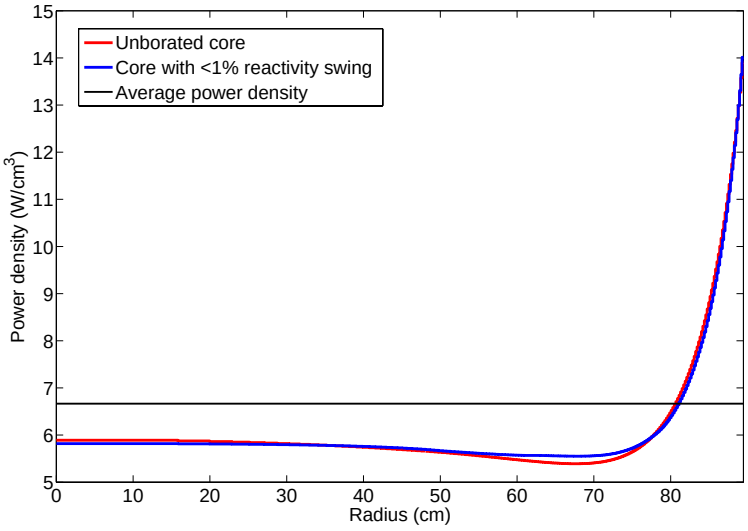


Figure 7.14: The power density in the radial directoin for an unborated core and a core with less than 1% reactivity swing at EOL

# Chapter 8

# Conclusion

## 8.1 Conclusions on reactor analysis

The adjoint function in the U-Battery has a different shape than the adjoint function in a PWR, while the forward spectrum is quite similar concerning the location of peaks and resonances. The difference is a dip in the fast region which is caused by the high amount of graphite in the reactor.

The change in $k_{eff}$ after insertion of poison is proportional to the product of the forward flux and the adjoint function. This peaks in the thermal region.

The reverse calculation based on equation 3.3 does not work, because:

- There is an interrelation of zones, which is unknown and changing for each change in the reactor. Even when the interrelation of the poison distribution, $\langle \Phi, \Phi^* \rangle \sim [B]$, is fixed the calculation does not work.

- The $\mathbf{M}$ operators determined in a time step puts a constraint on the $\mathbf{M}$ in the time step before this one. This constraint can only be communicated to the previous time step by an inverse burnup; the determination of the reactor mockup before depletion based on a range of fission products. This is very difficult as fission reactions produce products according to the "camel curve" [Duderstadt and Hamilton, 1976].

Another conclusion which can be drawn from the reverse calculation is that there will always be a shortening in lifetime. In the beginning of the last step the boron from the former step has not yet been burnt completely. There is too much boron left, so the $k_{eff}$ will be below one at this point. As the boron was distributed between the zones in such a way to have maximum burnup there will be an excess of boron in any configuration at this point and thus a shortening in lifetime.

## 8.2 Conclusions on parameter study

Several different configurations have been studied. The best results had the lowest $\Delta$k. This because the shortening in lifetime was inevitable as explained above.

### 8.2.1 Two variable approach

The two variable approach leads to three regions in which there is a $\Delta$k of less than 0.02. When the second parameter, the shortening in fuel lifetime, was taken into account, the region with a density between $6.10^{-4}$ and $7.10^{-4}$ in zone 3 and an atomic density of around $1.10^{-4}$ in zone 1 is the most favourable configuration. The most favoured calculated point with the lowest $\Delta$k in this region is the point with a density of $1.10^{-4}$ and $7.10^{-4}$ in zone 1 and 3 respectively. The reactivity swing at this point was 1.48% and it has a shortening in lifetime of 199 days. The design criteria are not met with this configuration.

When expanding this two variable approach to four variables it was found that the configuration with the lowest $\Delta$k, a reactivity swing of 1.31%, was found for a density of $1.10^{-4}$, $1.10^{-4}$, $2.10^{-4}$ and $12.10^{-4}$ in zone a, b, e and f respectively. The shortening in lifetime in this configuration is 165 days. Although the swing is lowered by this expansion it still isn't within the range set by the limitations.

### 8.2.2 Three variable approach

As the two variable approach did not give the desired result a three variable approach was done.

The initial calculation gave rise to a point where there was a low reactivity swing. Making a second grid refinement around this point an even lower reactivity swing was found. This swing has a $\Delta$k of 1.26% and a shortening in fuel lifetime of 134 days. This is still higher than the wanted $\Delta$k.

For a grid with six zones several solutions are possible with a reactivity swing below 1%. The densities for which the shortening of lifetime was lowest, 139 days, were densities of $5.10^{-5}$, $1.5.10^{-5}$, $2.5.10^{-5}$, $7.5.10^{-5}$, $4.10^{-4}$ and $8.10^{-4}$ for the zones a, b, c, d, e and f repectively.

### 8.2.3 Large core calculation

In the large core calculation a larger core was examined with a lower enrichment. From calculations done on this core it can be concluded that in the larger geometry a reactivity swing of just over 1% can be achieved with only the use of four zones. In this geometry

a shortening in lifetime can be avoided.

It can be seen that the larger core in the reference calculation needs four degrees of freedom (only four varied zones) while the small core needs at least six. This is due to the fact that the small core has a very high leakage in comparison with the large core, since the volume increases with $R^3$ and the surface with $R^2$. It can however be seen that in both cases a high density in the most outer zone is favoured, which indicates that a high suppression of uranium burnup is needed there in the beginning of life.

### 8.2.4 Wrap-up

From the above subsections it can be concluded that by the use of geometrical poison distribution a reactivity swing below 1% can be achieved. Achieving this without loss of fuel lifetime is not possible with the design freedoms investigated above. This was concluded as well from the reverse calculation in section 8.1. The shortening in lifetime will be discussed in the next chapter.

# Chapter 9

# Discussion and future work

## 9.1 TRISO coated particles

### 9.1.1 Particle production

The reactor concept presented in this thesis is still subject to change, however the features will roughly stay the same. The blending of the poison directly into the fuel zone of a TRISO coated particle has never been investigated. In order for the conclusions drawn in this thesis to hold, it should be verified in further experimental analysis whether this mixing is feasible. Especially the properties of such a TRISO have to be investigated in order to see if it can stay intact under the extreme conditions in a reactor. As this kind of experiments takes a long time (due to the irradiation research) it is questionable whether the concepts discussed in this thesis can be implemented before the U-Battery goes into production.

Another type of particle could be used as well to control the reactivity swing. Particles coated with a layer of boron should be investigated. The advantage of this type of particles is that the outer poison layer shields the burnup of the uranium inside the particle and saves it for a later point in the fuel lifetime.

### 9.1.2 Power peaking

It has been shown that the power peaking factor decreases when boron is inserted to control for over-reactivity at BOL. At the EOL however the power peaking factor is slightly higher for the borated core. It still needs to be evaluated if the calculated factor is low enough for a TRISO particle. This has to be done by calculating temperatures in different parts of the reactor and on a smaller scale by calculating temperatures in individual TRISO particles. Calculations have to be made where the neutronics and the thermal hydraulics are coupled as in this thesis and other U-Battery studies [De Zwaan, 2007] a constant fuel temperature has been used. Also a consideration has to be made to check if the distance between the different power densities is large enough. High power

density differences over small distances cause large temperature gradients, which cause material stresses.

## 9.2 Reverse calculation

The reverse calculation attempted in section 6 does not work for the chosen boron distribution. The three problems described in section 3.2 can be solved by:

- Iteratively run XSDRNPM to see what the effect is of boron insertion on the **M** matrix.
- Create a general fission product with averaged properties over all products produced in fission. With this general product it should be possible to predict the parent nuclides of this product.
- The interrelation between the zones should be solved for iteratively or a general leakage function should be derived, based on the properties of the different zones.

The above solutions need a lot of computing time due to the iterative routines that will be needed. In this thesis the computing power and time were limited. However attempts should be made in future work to evaluate the solutions above as every gain in fuel lifetime will increase the economic feasibility of the U-Battery. If an analytical approach is chosen in the last item the homogenisation used in the burnup script cannot be used as specific scatter and absorption data on the boundaries are needed in order to predict neutron behaviour for neutrons coming from a adjacent zone.

However it should be possible to create a line without discontinuities (i.e. the boron left after burnup matches the boron needed for the next time step) using a certain distribution as it has been shown in the results from the parameter study that a solution for which the $k_{eff}$ is between 0.99 and 1.01 is achievable. An approach to this can be iteratively changing the distribution between the zones.

## 9.3 Flux and adjoint function

In this thesis it is shown in a qualitative way that the product of the poison $\sigma_a$, the flux and adjoint function is a measure of the $\Delta k_{eff}$ obtained when inserting poison into a certain zone in the core, just as is expected from equation 4.7. This was done in a static way by only comparing a certain point in time (point just after samarium and xenon poisoning). Future work should include a quantitative analysis of the relation between the adjoint, the flux, the $\Delta k_{eff}$ and the insertion of boron. By doing this a prediction of the $\Delta k_{eff}$ can be made on the basis of a measured flux and adjoint and a certain amount of poison inserted.

Using the reverse calculation with fixed interrelations between the concentrations in different zones proportional to the product of the poison $\sigma_a$, the flux and adjoint function gives insight into the burnup of boron in a core. The distribution chosen shows that efficient burnup is not favourable in the first part of core life. Also the efficiency of burnup is not high enough at the end of fuel lifetime. Further investigation should include conducting a similar reverse calculation with inefficient burnup by distributing the poison not proportional to the product but inverse proportional to the product in order to "save" boron for later timesteps.

## 9.4 Parameter study

### 9.4.1 Reactivity swing

The parameter study shows that for different geometries with a four or six zone system a reactivity swing of less than 1% can be achieved. In a larger core geometry the number of zones needed to achieve such a low reactivity swing is smaller. This can be contributed to the fact that the leakage compared to volume is smaller for a large core.

### 9.4.2 Lifetime shortening

The shortening in fuel lifetime is however different for the two geometries studied. Avoiding shortening of lifetime in the small ($3m^3$) reactor was not possible. Minimising shortening of lifetime even more might be achieved by the use of burnable poison particles, as the macroscopic absorption cross section of these particles decreases quadratic in time [Dam, 2000a]. This is material for future study. In the large core there was no shortening in lifetime. This phenomenon is probably due to less leakage and should be investigated in future studies as well.

The shortening in fuel lifetime in the small core geometry however does not imply that the reactor is economically not attractive. The assumption made was that the thermal efficiency in the heat exchanger will not be enough below 923 °K to maintain the wanted power output. However below this temperature the reactor will still function but have a lower power output. The reactivity swing at the end of reactor lifetime is 1.3% below the line $k_{eff} = 1$. This implies an excess swing of 0.3%. From equation 2.4 this implies a temerature drop of 45 °K below the 923 degrees. When looking at the Carnot efficiency [Moran and Shapiro, 1998]

$$\eta_{max} = 1 - \frac{T_{cold}}{T_{hot}} \tag{9.1}$$

it can be seen that deviation from the minimum temperature (at a $T_{cold}$ of 298 °K) of 45 °K gives a change in maximum achievable efficiency from 0.68 to 0.66. This is a change in efficiency of around 1% which will give a change in maximum electrical power output of 1%. Further analysis will have to be done to assess whether this change is significant as a lot of other losses play a role in the thermal to electrical power conversion. This is

however a topic in the field of mechanical engineering and outside the scope of this thesis.

### 9.4.3 Reflector poisoning

The study shows that solutions for a low reactivity swing favour a high boron density in the outer zone. A small boron density is however needed in more internal zones. This could indicate that a certain high boron density in the reflector and a low boron density in the core could have a solution to the problem as well. As described in the introduction however it is not yet known whether the reflector will be used during several fuel batch loads. A first attempt was made to calculate what the influence of boron in the reflector will be. However the burnup scripts used in this thesis and the SCALE software [ORNL, 2005] do not allow depletion calculations in non-fuel zones. Masking the reflector as a fuel zone by the introduction of small amounts of uranium was used to assess the concept of introducing boron into the reflector. However the accuracy of the calculation method used needs to be investigated. In order to make accurate calculations modifications to the burnup script have to be done. These modifications include making the SCALE software accept depletion in a non-fuel zone.

From the calculations done towards reflector poisoning it can be seen that it is possible to get a reactivity swing below 1%. It can be seen that moving the large boron density from the outer zone into the reflector worsens the reactivity control when keeping a small density in zone 1. When however zone 3 is taken as a zone in the core which is poisoned, combined with poison in the reflector it can be seen that low reactivity swings can be achieved. This might be due to the fact that the poison in zone 3 not only has the effect of absorbing neutrons (which can be done in the reflector as well), but avoiding fission reactions in zone 3 as well. Further studies should be conducted towards reflector poisoning as optimization could lead to better results. Especially since the shortening of fuel lifetime seems to be less when poison is inserted into the reflector.

## 9.5 Alternative poisons

In this thesis boron was chosen as a burnable poison as many studies have already been conducted towards boron and boron is commonly used in reactivity control. There are however several other poisons which could be taken into consideration for use with the method of reactivity control developed in this thesis. Common poisons which should be taken into consideration are Cadmium-113 and Gadolinium-157. The cross sections of these poisons differ from each other and have different energy dependence which might give rise to other characteristics. The cross sections are shown in figure 4.3.

# Bibliography

H. van Dam. Long-term control of excess reactivity by burnable particles. *Annals of nuclear energy*, 27:733–743, 2000a.

H. van Dam. Long-term control of excess reactivity by burnable poison in reflector regions. *Annals of nuclear energy*, 27:63–69, 2000b.

S. De Zwaan. Parameter study u-battery. Delft University of Technology, January 2007.

James J. Duderstadt and Louis J. Hamilton. *Nuclear Reactor Analysis*. John Wiley, 1976.

R. Gontard and H. Nabielek. Performance evaluation of modern htr triso fuels. Technical Report HTA-IB-05/90, Forschungszentrum Julich, July 1990.

A.I. van Heek, M.M. Stempniewicz, D.F. da Cruz, and J.B.M. de Haas. Acacia: a small-scale power plant for near term deployment in new markets. *Nuclear Engineering and Design*, 234:71–86, 2004.

J.E. Hoogenboom and H. van Dam. *Kernreactorkunde*. Delft University of Technology, 1998.

J.L. Kloosterman. Application of boron and gadolinium burnable poison particles in uo2 and puo2 fuels in htrs. *Annals of Nuclear Energy*, 30:1807–1819, 2003.

Miachael J. Moran and Howard N. Shapiro. *Fundamentals of engineering thermodynamics*. Number ISBN 0 471 97960 0. John Wiley & Sons, 1998.

ORNL. *SCALE: A modular code system for performing standardized computer analysis for licensing evaluations, ORNL/TM-2005/39, version 5, Vols I-III*. Oak Ridge National Laboratories, April 2005. Available from Radiation Safety information Computational Center at Oak Ridge National Laboratory as CCC-725.

Karl O. Ott and Robert J. Neuhold. *Introductory Nuclear Reactor Dynamics*. Number ISBN: 0-89448-029-4. American Nuclear Society, 1985.

J.W. Sterbentz, B. Philips, R.L. Sant, G.S. Chan, and P.D. Bayless. Reactor physics parametric and depletion studies in support of triso particle fuel specification for the

next generation nuclear plant. Technical report ineel/ext-04-02331, Idaho National Engineering and Environmental Laboratory, Bechtel BWXT Idaho, LLC, September 2004.

Alberto Talamo. Managing the reactivity excess of the gas turbine-modular helium reactor by burnable poison and control rods. *Annals of Nuclear Energy*, 33:84–98, 2006.

G. van Uitert. The bbr, building block reactor. Alias Baby Reactor, January 2006.